



UNIVERSITÀ
DEGLI STUDI
FIRENZE

FLORE

Repository istituzionale dell'Università degli Studi di Firenze

Structural insights into the molecular function of human [2Fe-2S] BOLA1-GRX5 and [2Fe-2S] BOLA3-GRX5 complexes

Questa è la Versione finale referata (Post print/Accepted manuscript) della seguente pubblicazione:

Original Citation:

Structural insights into the molecular function of human [2Fe-2S] BOLA1-GRX5 and [2Fe-2S] BOLA3-GRX5 complexes / Veronica, Nasta; Andrea, Giachetti; Simone, Ciofi-Baffoni; Lucia, Banci. - In: BIOCHIMICA ET BIOPHYSICA ACTA-GENERAL SUBJECTS. - ISSN 0304-4165. - STAMPA. - 1861:(2017), pp. 2119-2131. [10.1016/j.bbagen.2017.05.005]

Availability:

The webpage <https://hdl.handle.net/2158/1083458> of the repository was last updated on 2021-03-29T23:21:29Z

Published version:

DOI: 10.1016/j.bbagen.2017.05.005

Terms of use:

Open Access

La pubblicazione è resa disponibile sotto le norme e i termini della licenza di deposito, secondo quanto stabilito dalla Policy per l'accesso aperto dell'Università degli Studi di Firenze (<https://www.sba.unifi.it/upload/policy-oa-2016-1.pdf>)

Publisher copyright claim:

La data sopra indicata si riferisce all'ultimo aggiornamento della scheda del Repository FloRe - The above-mentioned date refers to the last update of the record in the Institutional Repository FloRe

(Article begins on next page)

Structural insights into the molecular function of human [2Fe-2S]

BOLA1-GRX5 and [2Fe-2S] BOLA3-GRX5 complexes

Veronica Nasta^{a,b}, Andrea Giachetti^a, Simone Ciofi-Baffoni^{a,b}, Lucia Banci^{a,b,*}

^aMagnetic Resonance Center CERM, University of Florence, Via Luigi Sacconi 6, 50019, Sesto Fiorentino, Florence, Italy.

^bDepartment of Chemistry, University of Florence, Via della Lastruccia 3, 50019 Sesto Fiorentino, Florence, Italy.

*Corresponding author:

Prof. Lucia Banci; Phone: +39 055 4574273; Fax: +39 055 4574923; E-mail: banci@cerm.unifi.it

Abstract

Members of the monothiol glutaredoxin family and members of the BOLA-like protein family have recently emerged as specific interacting partners involved in iron-sulfur protein maturation and redox regulation pathways. It is known that human mitochondrial BOLA1 and BOLA3 form [2Fe-2S] cluster-bridged dimeric heterocomplexes with the monothiol glutaredoxin GRX5. The structure and cluster coordination of the two [2Fe-2S] heterocomplexes as well as their molecular function are, however, not defined yet. Experimentally-driven structural models of the two [2Fe-2S] cluster-bridged dimeric heterocomplexes, the relative stability of the two complexes and the redox properties of the [2Fe-2S] cluster bound to these complexes are here presented on the basis of UV/vis, CD, EPR and NMR spectroscopy and computational protein-protein docking. While the BOLA1-GRX5 complex coordinates a reduced, Rieske-type [2Fe-2S]⁺ cluster, an oxidized, ferredoxin-like [2Fe-2S]²⁺ cluster is present in the BOLA3-GRX5 complex. The [2Fe-2S] BOLA1-GRX5 complex is preferentially formed over the [2Fe-2S] GRX5-BOLA3 complex, as a result of a higher cluster binding affinity. All these observed differences provide the first indications discriminating the molecular function of the two [2Fe-2S] heterocomplexes.

Keywords: Iron-sulfur protein; GRX5; BOLA1; BOLA3; Iron metabolism; Glutaredoxin.

Abbreviations: glutaredoxins, Grxs; glutathione, GSH; wilde-type, wt; DTT, dithiothreitol; HSQC, Heteronuclear Single-Quantum Correlation.

1. Introduction

Monothiol glutaredoxins (Grxs), with a conserved CGFS active site, and BolA-like proteins have recently emerged as specific interacting partners [1-3]. This functional relationship is conserved in both prokaryotes and eukaryotes [4-7]. Bioinformatic analyses indicated that both genes are frequently adjacent in prokaryotic genomes, that some natural fusion proteins exist in a few microbes, and that there is a very strong gene co-occurrence of these genes [8,9]. Besides these genomic evidences, high-throughput approaches experimentally confirmed a physical interaction for *Homo sapiens*, *S. cerevisiae*, *Drosophila melanogaster*, *A. thaliana*, and *E. coli* Grxs and BolA proteins. From a functional perspective, a cytosolic Grx-BolA complex was found in yeast to be involved in a cytosolic-nuclear signaling pathway responsible of iron homeostasis regulation via two transcriptional activators Aft1 and Aft2 [10,11]. In humans, this cytosolic pathway is, however, not conserved and the homologous cytosolic heterocomplex has been shown to play a role in the maturation of cytosolic Fe/S proteins [12-14]. Similarly, mitochondrial yeast BolAs (i.e. BolA1 and BolA3) have been proposed to mature some [4Fe-4S] cluster proteins by playing a role in the late stages of Fe/S cluster insertion to target apo proteins [15,16]. In humans, BOLA3 is involved, similarly to yeast, in handling Fe/S centers for the maturation of some mitochondrial Fe/S binding enzymes such as the lipoate-containing 2-oxoacid dehydrogenases and the respiratory chain complexes [17-19]. On the contrary, BOLA1 has been implicated in the regulation of the mitochondrial thiol redox potential [20].

During the last years, Grx-BolA complexes have been spectroscopically and biochemically investigated in different organisms (*E. coli* [21,22], *A. thaliana* [23-25], *S. cerevisiae* [26,27], and humans [12,15,28]) indicating that the two proteins form a [2Fe-2S] cluster-bridged heterodimeric complex. However, no structures are yet available for the [2Fe-2S] cluster

bound form of any BolA-Grx dimeric complex. Only a NMR-based docking model of the apo GrxS14-BolA2 dimeric complex from *A. thaliana* is available [23].

BolA-like proteins are generally grouped into three subfamilies designated BolA1-, BolA2-, and BolA3-like proteins [29]. The genome of *H. sapiens* encodes three BolA homologues, one for each of the three subfamilies [2]. Multiple sequence alignment of prokaryotic and eukaryotic BolAs allowed to identify sequence patterns probably comprising the cluster ligands in human BOLAs, which are $\text{HX}_8\text{HX}_{18}\underline{\text{H}}\text{X}_{15}\mathbf{H}$ in BOLA1 and $\text{CX}_{21}\underline{\text{H}}\text{X}_{14}\mathbf{H}$ in both BOLA2 and BOLA3 (**Figure S1**). All prokaryotic and eukaryotic BolAs conserve the C-terminal histidine that is shown in bold in the above patterns. Spectroscopic data on Grx-BolA complexes from *E. coli*, *S. cerevisiae* and *A. thaliana* indicated that three ligands to the [2Fe-2S] cluster are provided by a conserved cysteine of monothiol Grx, by a GSH molecule bound to monothiol Grx, and by the invariant histidine at the C-terminus present in all BolA-like family members [22,23,28]. The nature of the fourth ligand in the *S. cerevisiae* heterocomplex still remains controversial, while spectroscopic data on *A. thaliana* and *E. coli* BolA1-like/Grx dimeric complexes indicated the presence of a Rieske-type [2Fe-2S] center with two His and two Cys ligands, both His suggested to be provided by the BolA protein. In humans, it is already well established that mitochondrial GRX5 binds the [2Fe-2S] cluster in both its homodimeric form and in the heterodimer with mitochondrial human BOLA1 and BOLA3, through the Cys residue (Cys 67) of the conserved CGFS motif and through a GRX5-bound glutathione (GSH) molecule [15,30,31]. The cluster ligands provided by BOLA1 and BOLA3 in the human heterodimeric complex are, on the contrary, not yet defined. Spectroscopic data are indeed available only for the cytosolic human [2Fe-2S] BOLA2-GRX3 dimeric complex, which showed the same cluster ligands found in the *S. cerevisiae* homologous heterocomplex [12,28]. Structural data on BOLA1 and BOLA3 can only exclude as a cluster ligand the histidine underlined in the above sequence patterns, because it is structurally far from all the other potential ligands [15,23,32-35].

Here, we investigated the [2Fe-2S] cluster coordination in the human BOLA1-GRX5 and BOLA3-GRX5 complexes by UV/vis, CD, EPR and NMR spectroscopy; we characterized the cluster redox properties and the relative stability of the two heterocomplexes; and we provided experimentally-driven structural models for the [2Fe-2S] cluster bound form of the two heterocomplexes. The present data provide structural and biochemical evidences contributing to the comprehension of the still poorly defined molecular function of these [2Fe-2S] heterocomplexes.

2. Materials and Methods

2.1 Protein production

Human glutaredoxin 5 (GRX5) (UniProtKB ID Q86SX6), human BOLA3 (BOLA3), and human BOLA1 (BOLA1) depleted of the N-terminal mitochondrial targeting sequence (GRX5, aa 1-34; BOLA3, aa 1-26; and BOLA1, aa 1-20) were produced as already reported [15,30].

Recombinant BOLA1 and BOLA3 mutants were obtained by site-directed mutagenesis (QuickChange Site-directed Mutagenesis Kit, Agilent Technologies) of pETG20A-BOLA3 and pET15-BOLA1 expression vectors, used for the production of wild-type (wt) proteins, by using primers containing the required single mutations, i.e. C59A and H96A for BOLA3, and H58A, H67A and H102A for BOLA1. Protein production of BOLA1 and BOLA3 mutants was obtained following the same procedure described for the wt proteins [15].

The [2Fe-2S] cluster bound forms of wt and mutant complexes were obtained by anaerobic chemical reconstitution of the apo heterocomplexes formed mixing apo GRX5 and BOLAs in a 1:1 ratio, obtained on the basis of NMR titration experiments (see section 2.4), by following a previously reported procedure [13].

2.2 Biochemical Methods

For GSH measurements, the chemically reconstituted Fe/S protein complexes in 50 mM phosphate buffer (pH 7.0) were denatured and precipitated with 5% (w/v) 5-sulfosalicylic acid, and GSH in the supernatant was measured using 5,5'-dithiobis(2-nitrobenzoic acid) and glutathione reductase by using Glutathione Assay Kit (Sigma-Aldrich). Protein concentrations of the hetero-complexes were determined by measuring absorbance at 280 nm of the apo proteins, which were then mixed at the 1:1 ratio and chemically reconstituted, using the extinction coefficients of the native proteins.

2.3 UV/visible, CD and EPR spectroscopy

UV/vis and CD absorption spectra were recorded under anaerobic conditions at room temperature in degassed 50 mM phosphate buffer (pH 7.0), 5 mM GSH, and 5 mM DTT, on a Cary 50 Eclipse spectrophotometer and JASCO J-810 spectropolarimeter, respectively. In the CD experiments, each sample was split into two aliquots, one containing degassed 50 mM phosphate buffer (pH 7), 5 mM GSH, and 5 mM DTT, and the other degassed 50 mM phosphate buffer (pH 7.0), in order to test GSH and DTT depletion effects. To investigate the redox properties of chemically reconstituted [2Fe-2S] BOLA1-GRX5 and [2Fe-2S] BOLA3-GRX5, UV/vis absorption and CD spectra were recorded under anaerobic conditions at room temperature in degassed 50 mM phosphate buffer (pH 7.0) in the presence of increasing amounts of dithionite, up to four electron equivalents. EPR spectra were recorded before and after anaerobic reduction of the cluster by stoichiometric addition of sodium dithionite and rapid freezing of the protein solution in liquid nitrogen. EPR spectra were acquired in degassed 50 mM phosphate buffer (pH 7.0), 5 mM GSH, 5 mM DTT, and 10% (v/v) glycerol at 45 K, using a Bruker Elexsys E500 spectrometer working at a

microwave frequency of ca. 9.45 GHz, equipped with a SHQ cavity and a continuous flow He cryostat (ESR900, Oxford instruments) for temperature control. Acquisition parameters were: microwave frequencies are specified in the figure captions; microwave power, 5 mW; modulation frequency, 100 kHz; modulation amplitude, 8.0 G; acquisition time constant, 163.84 ms; number of points 1024.

2.4 NMR spectroscopy

Paramagnetic ^1H NMR experiments of the chemically reconstituted [2Fe-2S] GRX5-BOLA1 and [2Fe-2S] GRX5-BOLA3 complexes were performed on a Bruker AVANCE600 spectrometer, equipped with a ^1H selective probe, and on a Bruker III HD AVANCE400 spectrometer, equipped with a PH ^1H selective 400SB probe, at 298 K and 283 K with protein samples in 50 mM phosphate (pH 7.0), 5 mM DTT, 5 mM GSH, 10% (v/v) D_2O . All diamagnetic NMR experiments were carried out at 298 K on a Bruker AVANCE700 spectrometer with 0.5-1 mM uniformly ^{15}N (or ^{13}C , ^{15}N) labeled or unlabeled protein samples in 50 mM phosphate (pH 7.0), 5 mM DTT, 5 mM GSH, 10% (v/v) D_2O . All NMR spectra were processed using the standard BRUKER software (Topspin 2.1) and analysed through the CARA program.

To follow the formation of the heterodimeric complex, ^{15}N -labeled apo BOLA1 or apo BOLA3 (wt or single mutants) samples were titrated with increasing amounts of unlabeled apo GRX5 till a 1:1 ratio was reached. Chemical shift changes were followed in the ^1H - ^{15}N HSQC NMR spectra, and the differences in chemical shifts between free and bound BOLAs in absence of 5 mM GSH, between the heterocomplexes before and after the addition of 5 mM GSH, and between the heterocomplexes complex before and after [2Fe-2S] cluster binding were mapped on the surface of the structural model of BOLAs [15]. To investigate the relative stability of the two [2Fe-2S] heterocomplexes, the following experiment was performed: ^{15}N -labelled BOLA3 was first titrated with ^{15}N -labelled BOLA1 up to a 1:1 protein ratio and ^1H -

¹⁵N HSQC NMR spectra were recorded, showing that the two proteins do not interact each other. This mixture was then titrated with unlabelled homodimeric [2Fe-2S] GRX5₂ up to a 1:1:2 protein ratio and chemical shift changes followed by ¹H-¹⁵N HSQC NMR spectra and compared with chemical shifts of the [2Fe-2S] GRX5-BOLA1 and [2Fe-2S] GRX5-BOLA3 complexes, obtained by mixing [2Fe-2S] GRX5₂ with BOLA1 or BOLA3 at a 1:1 ratio. These NMR data were also compared with ¹H-¹⁵N HSQC NMR spectra recorded on a titration performed mixing ¹⁵N-labelled BOLA3 with ¹⁵N-labelled BOLA1 at a 1:1 protein ratio with unlabeled apo GRX5 up to a final 1:1:2 ratio.

2.5 Molecular docking and energy minimization with AMBER force field

Structural models of the [2Fe-2S]¹⁺ GRX5-BOLA1 and [2Fe-2S]²⁺ GRX5-BOLA3 complexes were calculated using the protein-protein docking program HADDOCK 2.2 (high ambiguity driven protein-protein docking) by following the standard HADDOCK procedure [36]. Specifically, the structural models of the [2Fe-2S] GRX5-BOLAs dimers were built from the structures of individual proteins (GRX5 PDB entry 2WUL, BOLA3 PDB entry 2NCL and BOLA1 PDB entry 5LCI). The [2Fe-2S] cluster with a GSH molecule bound to GRX5 were taken from the X-ray structure of [2Fe-2S] GRX5₂ (PDB ID 2WUL, [31]), and included in the docking calculations. The [2Fe-2S] cluster in the appropriate redox state was bound to the BOLA1 and BOLA3 ligands using unambiguous distance restraints, while the GRX5 ligands (GSH and Cys) were included in the HADDOCK force field parametrization of the [2Fe-2S] cluster. The BOLA1 and BOLA3 ligands of the [2Fe-2S] cluster were selected on the basis of the mutagenesis and spectroscopic data. The NMR chemical shift mapping data, already available for the two wt heterocomplexes [15], were used to define ambiguous interaction restraints for the residues at the interface. The “active” residues were defined as those having a chemical shift perturbation upon complex formation larger than the average of $\Delta_{\text{avg}}(\text{HN})$ plus 1σ ($\Delta_{\text{avg}}(\text{HN}) = (((\Delta\text{H})^2 + (\Delta\text{N}/5)^2)/2)^{1/2}$, where ΔH and ΔN are chemical shift

differences for backbone amide ^1H and ^{15}N nuclei, respectively) and with a solvent accessibility higher than 50%; the “passive” residues were defined as those being surface neighbors to the active residues and with a solvent accessibility higher than 50%. The final ensemble of 200 solutions was analyzed and clustered based on the pair-wise RMSD matrix calculated over the backbone atoms of the interface residues of GRX5 after fitting on the interface residues of BOLA1 or BOLA3. This way of calculating RMSD values in HADDOCK results in high values that emphasize the differences between docking solutions. For this reason, clustering was performed using a 7.5 Å cut-off. In the case of BOLA1-GRX5 complex, the docking calculations were performed considering that His 67 and His 102 can coordinate the iron through N δ 1 or N ϵ 2, thus generating four docking results. After final refinement in water, the docked structures were clustered using the standard HADDOCK algorithm and the HADDOCK scores in the four docking calculations compared (**Table S1**). It resulted that the model, where N δ 1 of His 67 and N ϵ 2 of His 102 coordinate the iron ions, provides the best cluster binding mode on the basis of the HADDOCK score (**Table S1**). Applying the same approach to select the coordination mode of His 96 in [2Fe-2S] BOLA3-GRX5, it resulted that the best-scoring binding mode is that where N δ 1 of His 96 binds the iron (**Table S1**). The docking calculations of the best-scoring His binding modes for the two heterocomplexes yielded 4 clusters for BOLA3-GRX5 and BOLA1-GRX5 complexes (**Table S2**). The best-scoring HADDOCK cluster for each heterocomplex resulted the most populated, with 155 structures, for BOLA1-GRX5, and 148 structures, for BOLA3-GRX5, out of the 200 calculated structures, indicating that they represent the most reliable solutions (**Table S2**). The clusters were ranked based on the averaged HADDOCK score of their top four members. For the [2Fe-2S] $^{1+}$ GRX5-BOLA1 and [2Fe-2S] $^{2+}$ GRX5-BOLA3 complexes, the best structure with the highest HADDOCK scoring cluster was then energy minimized in explicit water, using AMBER molecular dynamics program [37]. AMBER force field

parametrization of the [2Fe-2S] cluster was obtained using a python based metal center parameter builder [38].

3. Results and Discussion

3.1 NMR and EPR reveal different redox states for the two [2Fe-2S] BOLA1-GRX5 and [2Fe-2S] BOLA3-GRX5 complexes

Paramagnetic ^1H NMR and EPR spectroscopy were used to characterize the redox state of the [2Fe-2S] cluster for the two dimeric BOLA1-GRX5 and BOLA3-GRX5 complexes. EPR data showed that the BOLA3-GRX5 complex chemically reconstituted in strictly anaerobic conditions with a [2Fe-2S] cluster was EPR silent, as expected for the presence of a $S = 0$ ground state in an oxidized $[\text{2Fe-2S}]^{2+}$ cluster, while, for the BOLA1-GRX5 complex, also chemically reconstituted in strictly anaerobic conditions with a [2Fe-2S] cluster, an EPR signal typical of a $S = 1/2$ reduced $[\text{2Fe-2S}]^{1+}$ center was observed (**Figure 1A** and **1B**). By adding dithionite to the [2Fe-2S] BOLA3-GRX5 complex, the EPR spectrum of a $S = 1/2$ $[\text{2Fe-2S}]^{1+}$ cluster appears (**Figure 1A**). Paramagnetic ^1H NMR spectrum of the [2Fe-2S] BOLA3-GRX5 complex showed the presence of broad signals at 37, 32 and 23 ppm and a sharper one at 14 ppm (**Figure 1C**), all of them typical of an oxidized $[\text{2Fe-2S}]^{2+}$ cluster-containing species [39]. In conclusion, both EPR and NMR data of the BOLA3-GRX5 complex indicate that the [2Fe-2S] cluster is in the oxidized state. On the contrary, the NMR spectrum of the [2Fe-2S] BOLA1-GRX5 complex at 600 MHz and 283 K showed the presence of two broad down-field shifted peaks at about 92 and 88 ppm and sharper peaks at 44 and 29 ppm, together with up-field shifted sharp signals at -4.3 and -6.0 ppm (**Figure 1D**). Paramagnetic ^1H NMR spectrum of [2Fe-2S] BOLA1-GRX5, acquired at a lower magnetic field (400 MHz) and higher temperature (298 K), showed the presence of two additional down-field shifted broad peaks at 77 and 110 ppm (**Figure S2**). These down-field

shifted signals exhibited Curie-type temperature dependence (viz., the high-frequency-shifted peaks move to lower frequency, toward their diamagnetic positions, as the temperature is raised); consistently, the up-field shifted signals have pseudo-Curie-type temperature dependence (viz., the low-frequency-shifted peaks move to higher frequency, toward their diamagnetic positions, as the temperature is raised) [39,40]. Both the observed chemical shift pattern and the temperature dependence of the NMR signals indicate the presence of a reduced $[2\text{Fe-2S}]^{1+}$ cluster in the BOLA1-GRX5 complex.

The redox properties of the $[2\text{Fe-2S}]^{2+/1+}$ centers in the two heterocomplexes were investigated titrating the chemically reconstituted complexes with dithionite and the reaction followed by UV-vis and CD spectroscopy. The reduced $[2\text{Fe-2S}]^{1+}$ state of the cluster in the BOLA3-GRX5 complex is not stable, as it was destroyed upon dithionite treatment with no residual visible and CD peaks (EPR spectra discussed above were obtained only by rapidly freezing the sample once treated with stoichiometric dithionite additions). The $[2\text{Fe-2S}]^{2+}$ cluster in BOLA3-GRX5 behaves similarly to CGFS-Grxs homodimers which are both oxidatively and reductively labile [41]. Thus, BOLA3-GRX5, similarly to CGFS-Grxs homodimers, are unlikely to be redox active *in vivo*, but likely act as cluster transfer protein. On the contrary, a slight decrease of the molar absorptivity in the UV-vis spectra upon sub-stoichiometric dithionite additions was observed in the $[2\text{Fe-2S}]$ BOLA1-GRX5 complex and further additions of dithionite up to four electron equivalents do not perturb anymore molar absorptivity (**Figure S3**). The CD spectra are also slightly perturbed upon dithionite additions (**Figure S3**). These data indicate that a small fraction of the cluster bound to the complex is in the oxidized $[2\text{Fe-2S}]^{+2}$ state and that dithionite can completely reduce the cluster without promoting cluster degradation, at variance of what observed for the $[2\text{Fe-2S}]$ BOLA3-GRX5 complex. The presence of a small percentage of oxidized $[2\text{Fe-2S}]^{+2}$ cluster in the chemically reconstituted $[2\text{Fe-2S}]$ BOLA1-GRX5 complex is also visible in the paramagnetic NMR spectrum, which shows very weak peaks typical of the oxidized $[2\text{Fe-2S}]^{2+}$ cluster-containing

species (**Figure 1**). In conclusion, the [2Fe-2S] center in the BOLA1-GRX5 complex behaves like a stable redox active center able to perform electron transfer reactions to dithionite. This result supports a possible physiological role of the [2Fe-2S] BOLA1-GRX5 complex in electron transfer reactions. Moreover, the EPR and NMR data indicates that the two BOLAs stabilize different redox states of the [2Fe-2S] cluster in anaerobic conditions, i.e. BOLA1 essentially stabilizes a reduced [2Fe-2S]¹⁺ cluster and BOLA3 an oxidized [2Fe-2S]²⁺ cluster. On the basis of literature data that reported higher redox potentials for a [2Fe-2S] cluster coordinated by a higher number of His ligands with respect to Cys ligands [42], we could suggest different cluster ligands in the two heterodimeric complexes, i.e. BOLA1 having a higher number of His as cluster ligands than BOLA3.

3.2 Spectroscopic studies to investigate BOLAs cluster ligands in the [2Fe-2S] BOLA1-GRX5 and [2Fe-2S] BOLA3-GRX5 dimeric complexes

Literature data available on [2Fe-2S] BolA-Grx complexes showed that the invariant C-terminal His of BolAs (His 96 in BOLA3 and His 102 in BOLA1) is a cluster ligand [2,12,22,23,26-28]. However, the other BolA ligand in the BolA1-like and BolA3-like heterocomplexes still remains elusive. Multiple amino acid sequence alignments of BolA1-like and BolA3-like subfamilies (**Figure S1**) can provide information on the missing cluster ligand in human BOLA1 and BOLA3. Specifically, while BOLA3 has only another possible cluster ligand (Cys 59), BOLA1 has two highly conserved His residues (His 58 and His 67), which are both structurally close to the invariant C-terminal His ligand (His 102), suggesting that either His 58 or His 67 might be a cluster ligand. In order to test whether Cys 59 in BOLA3, and His 58 or His 67 in BOLA1 are involved in [2Fe-2S] cluster binding, we generated a number of single Cys/His-to-Ala mutations in BOLA3 and BOLA1 to gauge how elimination of each putative metal-binding residue influences the BOLA1 (or BOLA3)-GRX5 complex formation and the cluster binding.

UV/vis, CD, NMR and EPR spectroscopy were applied on these mutant complexes to identify BOLA1 and BOLA3 ligands in wt [2Fe-2S] BOLA1-GRX5 and wt [2Fe-2S] BOLA3-GRX5 dimeric complexes. Before doing this, we have established whether the mutations affect the number of GSH molecules per heterocomplex, following a standard approach [43]. From these data (**Table S3**), it resulted that chemically reconstituted wt BOLA1-GRX5, H58A BOLA1-GRX5, wt BOLA3-GRX5 and C59A BOLA3-GRX5 bind one GSH molecule per heterocomplex. These results suggest that the GSH molecule interacting at the GSH binding site of GRX5 [30,31] is bound to the cluster in these complexes, and that H58 and C59 mutations do not promote the binding of further GSH molecules to the cluster. On the contrary, the [2Fe-2S] H67A BOLA1-GRX5 complex binds more than one GSH molecule per heterocomplex, i.e. ~1.3 GSH:heterocomplex (**Table S3**). These data suggest that about 30% of the [2Fe-2S] H67A BOLA1-GRX5 molecules binds a further GSH molecule to the cluster.

The heterodimeric complexes of any BOLA1 and BOLA3 mutants with GRX5 were still able to bind a [2Fe-2S] cluster, as indicated by UV/vis spectra (**Figure 2**). Specifically, the UV/vis spectra of the [2Fe-2S] H58A and H67A BOLA1-GRX5 complexes are comparable with that of the wt heterocomplex, although the relative intensities of the bands in the visible region between 350 and 700 nm are different (**Figure 2A**). From these spectra it is not possible to discriminate which between His 58 and His 67 of BOLA1 is the cluster ligand. On the contrary, the UV/vis spectrum of [2Fe-2S] C59A BOLA3-GRX5 significantly differs from the wt one (**Figure 2B**), indicating an apparent change in the interaction between the [2Fe-2S] cluster and the protein upon Cys 59 mutation, thus suggesting that Cys 59 of BOLA3 might be involved in cluster binding. Moreover, the UV/vis spectrum of human C59A BOLA3-GRX5 is very similar to those of human BOLA2-GRX3 [12,28] and yeast Fra2-Grx3 complexes [26,27], consistent with the same coordination pattern, which has been identified in human BOLA2-GRX3 and yeast Fra2-Grx3 complexes to be one His from Fra2/BOLA2, one Cys

from Grx3/GRX3, one GSH molecule and an undefined N/O ligand [26-28]. On this basis, the difference observed in the UV/vis spectra among wt and C59A BOLA3 heterocomplexes support a model in which BOLA3 involves the conserved Cys 59 in cluster binding, in addition to the invariant C-terminal histidine.

CD spectra were recorded for all wt and BOLA mutant complexes in phosphate buffer in the presence or not of 5 mM DTT and 5 mM GSH, in order to monitor possible effects of S-donor small molecules on cluster coordination in the heterocomplexes. From these data, it resulted that CD spectra of wt BOLA1 and wt BOLA3 complexes are not significantly affected by the presence of 5 mM DTT and 5 mM GSH (**Figure 3A**), suggesting that cluster coordination is not modified by the presence of S-donor small molecules. Also the CD spectrum of [2Fe-2S] H58A BOLA1-GRX5 complex is not significantly affected by the presence of S-donor small molecules (**Figure 3A**), indicating that the [2Fe-2S] cluster coordination in this complex is not modified by the presence of S-donor small molecules. According to this, the His 58 mutation does not promote the binding of further GSH molecules (i.e. only one GSH molecule per [2Fe-2S] H58A BOLA1-GRX5 complex, as found in [2Fe-2S] BOLA1-GRX5 complex, **Table S3**). The variations in the CD spectra between the [2Fe-2S] wt heterocomplex and the [2Fe-2S] H58A heterocomplex (**Figure 3A**) can be thus ascribed to a change in the cluster environment due to the structural proximity of His 58 to the [2Fe-2S] cluster. This interpretation is in agreement with the structural model of [2Fe-2S] BOLA1-GRX5 complex (see section 3.4). The CD spectrum of [2Fe-2S] H67A BOLA1-GRX5 complex is slightly affected by the presence of DTT and GSH, and more closely matches that of [2Fe-2S] BOLA1-GRX5 heterocomplex in the buffer not containing 5 mM DTT and 5 mM GSH. These effects suggest that S-donor small molecules might contribute to cluster coordination in the H67A BOLA1-GRX5 heterocomplex. The presence of more than 1 eq. of GSH per [2Fe-2S] H67A BOLA1-GRX5 heterocomplex also supports this model, indicating that GSH can be the participating S-donor ligand. The GSH additional

contribution to cluster coordination is, however, is not quantitative, as we estimated that only about 30% of the [2Fe-2S] H67A BOLA1-GRX5 heterocomplex contains two GSH molecules (**Table S3**) providing a 2GSH-Cys 67(GRX5)-His 102(BOLA1) cluster coordination for only a ~30% of the complex. These data therefore suggest that His 67 is a cluster ligand, although they do not address which is the preferential ligand replacing His 67 once it is mutated. The CD spectrum of [2Fe-2S] C59A BOLA3-GRX5 is also slightly perturbed by the presence of S-donor small molecules (**Figure 3B**), suggesting that cluster coordination might be modified by the presence of S-donor small molecules. However, [2Fe-2S] C59A BOLA3-GRX5 binds one GSH molecule per heterocomplex (**Table S3**), similarly to [2Fe-2S] BOLA3-GRX5 complex, and the CD spectrum of [2Fe-2S] BOLA3-GRX5 complex does not more closely match the CD spectrum of [2Fe-2S] C59A BOLA3-GRX5 in both GSH/DTT containing and not-containing buffers, at variance with what observed for the [2Fe-2S] H67A BOLA1-GRX5 complex. Therefore, the GSH/DTT-dependent changes observed in the CD spectra of [2Fe-2S] C59A BOLA3-GRX5 cannot conclusively attributed to the direct participation of a further GSH/DTT molecule to cluster binding, but most likely to a perturbation on the cluster binding site region induced by the presence or not of GSH/DTT molecules. This result suggests that the cluster is more solvent exposed in [2Fe-2S] BOLA3 heterocomplex than in [2Fe-2S] BOLA1 heterocomplex. According to this view, the CD spectrum of [2Fe-2S] BOLA1 heterocomplex is completely unperturbed over different buffer conditions, while that of [2Fe-2S] WT BOLA3 heterocomplex shows small differences in signal intensity of the bands at 465 and 567 nm upon different buffer conditions. To define whether the C59A mutation has an real effect on the cluster binding region, we need therefore to compare the CD spectra of [2Fe-2S] C59A BOLA3-GRX5 versus that of [2Fe-2S] BOLA3-GRX5 complex performed in the same buffer (i.e. buffer not containing 5 mM DTT and 5 mM GSH, **Figure 3B**). Some differences between them were observed, indicating that Cys 59 is close to the [2Fe-2S] cluster in such a way that its mutation

influences the coordination environment of the cluster. In conclusion, UV/vis and CD data suggest that Cys 59 might be a cluster ligand in the [2Fe-2S] BOLA3-GRX5 complex, but does not provide a clear picture of which between His 58 and His 67 of BOLA1 is the cluster ligand in the [2Fe-2S] BOLA1-GRX5 complex. NMR spectroscopy was therefore applied on both complexes to provide more definitive information.

By analyzing ^1H - ^{15}N NMR backbone chemical shift differences between wt BOLAs and their mutants (**Figure 4**), it resulted that: i) the C59A mutation in BOLA3 affects only a few residues of the loop containing the mutation; ii) either H58A or H67A mutations in BOLA1 affect, in addition to residues of the region containing the mutation, the invariant C-terminal His 102, and the region around the other, not mutated histidine. These results are in agreement with what can be predicted from the solution structures of the two apo proteins [15], which showed that Cys 59 of BOLA3 is highly solvent exposed and thus not in contact with other protein regions, while His 58 and His 67 in BOLA1 are close each other as well as to His 102.

NMR titrations of ^{15}N -labeled apo BOLA1 or BOLA3 mutants with unlabeled apo GRX5 were then performed, and, from ^1H - ^{15}N HSQC spectra analysis, it resulted that the BOLAs mutants behave like the wt protein in forming a 1:1 apo heterocomplex with GRX5, and in having a GSH molecule bound to the complex. Comparing the chemical shift differences of BOLA1- or BOLA3-GRX5 heterocomplexes with those of their respective mutants, similar interaction regions were indeed identified (**Figure 5A** and **6A**). Also GSH addition affects backbone chemical shifts in similar regions for wt and mutants complexes (**Figure 5B** and **6B**). In the case of the H67A BOLA1 mutant, even if the interacting region is the same as that in the wt protein, the residues affected by the interaction with GRX5 and by GSH binding are, however, scattered and less residues show meaningful chemical shift differences (**Figure 6A** and **6B**). In conclusion, structurally similar apo heterocomplexes are formed by wt and BOLAs mutants. In order to learn about BOLA1 and BOLA3 cluster ligands in the

heterocomplexes, the effects of the various mutations on the backbone chemical shifts of the residues close to the paramagnetic [2Fe-2S] center of the heterocomplexes were explored by NMR. Specifically, a comparison of the backbone chemical shift values of BOLA1 and of BOLA3 in the apo heterocomplex versus BOLA1 and BOLA3 in the [2Fe-2S] cluster bound heterocomplex was performed for each BOLA1 and BOLA3 mutant and for the wt proteins. Meaningful chemical shift changes were then mapped on the BOLA1 and BOLA3 structures (**Figures 5C** and **6C**). By analyzing them it resulted that: i) [2Fe-2S] cluster binding affects much fewer residues of the loop containing Cys 59 of BOLA3 when this Cys is mutated to Ala than in wt protein (**Figure 5C**); ii) [2Fe-2S] cluster binding affects His 67 of BOLA1 and surrounding residues, when His 58 is mutated to Ala (i.e. broadening beyond detection effects observed for these residues), as it occurs for wt protein, while the mutated His 58 region in both H58A BOLA1 and wt protein does not show broadening beyond detection effects (**Figure 6C**); iii) [2Fe-2S] cluster binding affects at a similar extent both His 67 and His 58 regions (broadening beyond detection effects were observed for both regions) when His 67 is mutated to Ala, at variance with what occurs in wt BOLA1 whose His 58 region does not display broadening beyond detection as well as no meaningful chemical shift changes (**Figure 6C**); iv) [2Fe-2S] cluster binding affects the region containing the invariant C-terminal His in all mutants in a similar manner as observed for wt, i.e. broadening beyond detection is observed in this region (**Figure 6C**). Overall, these results indicate that Cys 59 of BOLA3 is involved in [2Fe-2S] cluster binding in the wt [2Fe-2S] heterocomplex, that His 67 of BOLA1 is involved in [2Fe-2S] cluster binding in both H58A mutant and wt [2Fe-2S] heterocomplexes, and that His 58 can substitute His 67 in ligating the cluster once the latter His is mutated to Ala. Finally, the NMR data indicate that the invariant C-terminal His is involved in cluster binding in all these heterocomplexes.

EPR spectra on the [2Fe-2S] cluster-bound forms of the mutated heterocomplexes were compared with those of the wt heterocomplexes, with the assumption that the mutations are

not drastically perturbing the electronic delocalization. They showed that, as it occurs for the wt heterocomplexes (see section 3.1), the C59A BOLA3-GRX5 complex is EPR silent (**Figure 7A**), while an EPR signal was observed in the H58A and H67A BOLA1-GRX5 complexes (**Figure 7B** and **7C**), indicating that the mutations do not drastically modify the cluster redox state of the GRX5-BOLA1 and GRX5-BOLA3 complexes, i.e. reduced $[2\text{Fe-2S}]^{1+}$ and oxidized $[2\text{Fe-2S}]^{2+}$, respectively. Both $[2\text{Fe-2S}]$ H58A BOLA1-GRX5 and $[2\text{Fe-2S}]$ H67A BOLA1-GRX5 complexes exhibit nearly axial EPR signals, as in the wt heterocomplex, with the same g_{av} of 2.00 and very similar anisotropy (**Figure 1B**, and **Figure 7B** and **7C**). These results suggest an invariant coordination pattern for all $[2\text{Fe-2S}]$ BOLA1-GRX5 complexes, indicating that, once His 67 is mutated, the nearby His 58 can coordinate the $[2\text{Fe-2S}]$ cluster. In this respect, the EPR data are in full agreement with the NMR data described above and support the same conclusion. However, considering GSH quantification data showing that the $[2\text{Fe-2S}]$ H67A BOLA1-GRX5 complex binds slightly more than one GSH per heterodimer (**Table S3**) and the influence of S-donor small molecules on the CD spectrum of H67A BOLA1-GRX5 complex (**Figure 3A**), a competitive ligand equilibrium between GSH molecules and His 58 in coordinating the same iron ion of the cluster can act once His 67 is mutated. This equilibrium is not present in the wt heterocomplex, as its CD spectrum is totally unaffected by S-donor small molecules (**Figure 3A**) and only one GSH molecule is present per heterodimeric complex (**Table S3**). Dithionite reduction of the $[2\text{Fe-2S}]$ C59A BOLA3-GRX5 complex provides EPR signals typical of a $S = 1/2$ $[2\text{Fe-2S}]^{1+}$ center (**Figure 7A**). The signals of the reduced $[2\text{Fe-2S}]$ C59A BOLA3-GRX5 complex are very different from those observed for the $[2\text{Fe-2S}]^{1+}$ center in the wt heterocomplex, being the resonance nearly axial with $g_{\perp} > g_{\parallel}$ in wt BOLA3-GRX5 complex and rhombic in C59A BOLA3-GRX5 complex, and being the g_{av} decreased from 2.00 to 1.93. This decrease in the g_{av} is in agreement with a S-ligand being replaced by a N/O-ligand [44], indicating that Cys 59 is a cluster ligand in $[2\text{Fe-2S}]$ wt BOLA3-GRX5, consistent

with the Uv/vis, CD and NMR data described above. Moreover, the EPR spectrum of the [2Fe-2S] C59A BOLA3-GRX5 complex shows the same rhombicity and g_{av} value as that of yeast [2Fe-2S] Fra2-Grx3 complex, which has been shown to not involve any Cys of Fra2 in cluster binding [26]. Therefore, the two systems (C59A BOLA3-GRX5 and Fra2-Grx3) acquire the same coordination pattern, i.e. a Cys and GSH molecule from the Grx moiety, a His from BOLA3 or from Fra2, and an undefined N/O-ligand. This comparison further support that Cys 59 is a cluster ligand in [2Fe-2S] BOLA3-GRX5 complex.

The g_{av} values of human BOLAs-GRX5 complexes (wt and mutant BOLAs) are higher than expected from literature data on similar systems [22,23,26,28]). Taking into account that NMR measurements indicate that human BOLAs-GRX5 complexes bind a [2Fe-2S] cluster through 2 Cys and 2 His ligands in BOLA1 and through 3 Cys and 1 His ligands in BOLA3, this behavior can be rationalized considering that, once the two iron ions of the [2Fe-2S]¹⁺ cluster have a fully or partial delocalized electronic distribution for the unpaired electron, then the cluster exhibits a larger g_{av} value than for an electronically localized system, which favors a smaller g_{av} value [45]. On this basis, a partial delocalized electronic distribution is expected to be present in the human [2Fe-2S]¹⁺ BOLAs-GRX5 complexes, thus determining an increase in the g_{av} values. A similar increase in the g_{av} values than expected from a valence-localized model was also observed for *E. coli* BolA-Grx4 [22], yeast Fra2-Grx3 [26] and human GRX3-BOLA2 [28]. In these cases, indeed, experimentally determined g_{av} values of ~1.93 were higher than those expected for the 2His-2Cys (g_{av} ~1.90) and 1His-1N/O-2Cys (g_{av} ~1.90) coordinations, which were, respectively, proposed for the *E. coli* BolA-Grx4 and yeast/human Fra2-Grx3/GRX3-BOLA2 heterocomplexes, on the basis of other spectroscopic techniques.

The invariant C-terminal His in yeast BolA1 and BolA3 has been shown to be important for the respiratory growth of cells, suggesting that it might be a potential cluster ligand [16]. Those observations agree with the NMR data here presented on human BOLA1 and BOLA3

[2Fe-2S] complexes, showing that this His is a cluster ligand. On the contrary, mutation of His 56 (corresponding to His 67 in BOLA1) to Ala or Lys in yeast BOLA1 failed to yield a significant yeast phenotype, suggesting that His 56 should not contribute to the Fe/S cluster binding [16], at variance with what proposed here for the corresponding His 67 in the human [2Fe-2S] BOLA1-GRX5 complex. Similarly, mutation of Cys 64 (corresponding to Cys 59 in BOLA3) to Ala or Lys in yeast BOLA3 failed to yield a significant yeast phenotype, thus potentially Cys 64 not contributing to the Fe/S cluster binding, at variance again with what proposed here for the corresponding Cys 59 in the human [2Fe-2S] BOLA3-GRX5 complex. Since we think reasonable that the yeast and human heterocomplexes should have the same cluster ligands, as the same metal binding pattern is conserved in the sequence of both organisms, we need to rationalize these potentially conflicting *in vivo* vs. *in vitro* results. We propose that a mutation of the invariant C-terminal His plays a role in cluster binding more critical than mutations of the other ligands (Cys 59 in human BOLA3 or Cys 64 in yeast BOLA3; His 67 in human BOLA1 or His 56 in yeast BOLA1), similarly to what was observed in *E. coli* Grx4-IbaG complex, in which the invariant C-terminal His is more important than His 27 (corresponding to His 67 in BOLA1) for stabilizing the [2Fe-2S] cluster-bound heterodimer complex [22]. Thus, at cellular level, the mutation on the invariant C-terminal His is expected to be the determinant factor for observing significant phenotype effects with respect to the other mutations. To investigate such hypothesis, we produced His to Ala mutants of the invariant C-terminal His in BOLA1 and BOLA3, i.e. H102A BOLA1 and H96A BOLA3, and investigated their cluster binding properties once complexed with GRX5. Both H102A BOLA3 and H96A BOLA1 mutant still forms a [2Fe-2S] bound complex with GRX5 upon chemical reconstitution, similarly to what was observed in the homologous yeast H103A Fra2-Grx3 complex [27]. The UV/vis spectra of H102A BOLA1-GRX5 and H96A BOLA3-GRX5 complexes are indeed typical of the presence of a [2Fe-2S] bound cluster (**Figure S4**). ¹H-¹⁵N HSQC spectra acquired on the [2Fe-2S] bound form of these

heterocomplexes showed, however, the presence of a double set of cross-peaks in an equimolar ratio for several backbone NHs of BOLA1 or BOLA3 residues, indicating the presence in solution of two [2Fe-2S] BOLAs conformations. These conformations might originate from cluster-ligand exchange equilibria caused by the lack of the invariant C-terminal His ligand. This conclusion is supported by what has been observed in the homologous *E. coli* Grx4-IbaG complex, which binds two GSH molecules per [2Fe-2S] cluster, once the C-terminal His was mutated, at variance with the wt heterocomplex that binds one GSH per [2Fe-2S] cluster [22]. The observation of a double set of cross-peaks in the NMR spectra, corresponding to the different conformations, has not been observed for all other [2Fe-2S] heterocomplexes involving either the wt proteins or the other mutants of BOLA1 and BOLA3. Therefore, the invariant His plays a crucial role in structurally stabilizing the [2Fe-2S] heterocomplexes in a unique cluster bound conformation. Accordingly to the role of the invariant His in stabilizing cluster binding, we observed that, once [2Fe-2S] H102A BOLA1-GRX5 and [2Fe-2S] H96A BOLA3-GRX5 complexes were reduced by dithionite, the [2Fe-2S] cluster was highly unstable, readily degrading as evidenced by irreversible bleaching of the UV/vis absorption spectra and by the absence of an EPR signal corresponding to a $S = 1/2$ [2Fe-2S]¹⁺ center, at variance with what occurs for the wt and all the other mutant heterocomplexes. The conformational variability observed for the H96A and H102A BOLA1 mutant heterocomplexes can therefore explain the observed cluster instability upon reduction, once the invariant C-terminal His is mutated. The same behavior has been reported for the yeast [2Fe-2S] Grx3-Fra2 complex, which involves in cluster binding the C-terminal invariant His 103. Once His 103 of Fra2 was mutated to Ala or Cys, EPR and UV/vis data clearly demonstrate that the [2Fe-2S] cluster is relatively unstable to reduction [27].

The failure to observe a significant yeast phenotype once His 56 is mutated to Ala or Lys in yeast BOLA1, could be also rationalized considering that the H67A BOLA1 mutant binds a

[2Fe-2S] cluster in the heterodimer with GRX5 by substituting, as cluster ligand, the mutated His 67 with the nearby His 58. This ligand substitution determines that cluster binding and redox properties of the protein are not largely affected by the mutation, and thus no significant phenotype is expected to be observed.

3.3 Interaction of [2Fe-2S] GRX5₂ with BOLA3 and BOLA1

We have previously shown that apo GRX5 has a similar affinity for BOLA3 and BOLA1. Apo GRX5 is indeed equally partitioned in solution between the two BOLA1 and BOLA3 proteins upon its addition to a 1:1 BOLA1-BOLA3 mixture [15]. Once a 1:1:2 BOLA1-BOLA3-GRX5 protein ratio was reached, both apo 1:1 heterodimeric complexes are completely formed with no free apo GRX5 present in solution [15]. We have here investigated whether the binding of the [2Fe-2S] cluster to the two apo heterocomplexes can favor the formation of one vs. the other complex, i.e. [2Fe-2S] GRX5-BOLA1 vs. [2Fe-2S] GRX5-BOLA3. To address this question, a 1:1 ¹⁵N-labelled apo BOLA3-¹⁵N-labelled apo BOLA1 mixture was titrated with unlabelled homodimeric [2Fe-2S] GRX5₂ up to a 2:1:1 [2Fe-2S] GRX5₂-BOLA1-BOLA3 protein ratio. Following the titration through ¹H-¹⁵N HSQC NMR spectra, we observed the almost complete formation of the [2Fe-2S] GRX5-BOLA1 complex once one equivalent of [2Fe-2S] GRX5₂ was added to the protein mixture, while the [2Fe-2S] GRX5-BOLA3 complex was still not formed. Specifically, some BOLA1 residues, such as that of Ala 94, shown in **Figure S5**, display chemical shift changes in a slow exchange regime on the NMR time scale between free BOLA1 protein and the complexed BOLA1 in [2Fe-2S] GRX5-BOLA1 during the additions of [2Fe-2S] GRX5₂ up to a 1:1:1 protein ratio, and they indicate an almost quantitative formation of the latter complex once the 1:1:1 ratio is reached between the three proteins (**Figure S5**). On the contrary, the chemical shifts of some residues of BOLA3, i.e. the residues of the Cys binding loop, show exclusively chemical shifts changes in a fast exchange regime on the NMR time scale (**Figure S5**). These fast

exchange chemical shift changes match those observed by titrating a 1:1 mixture of ^{15}N -BOLA1 and ^{15}N -BOLA3 with apo GRX5 (**Figure S5**), indicating that upon addition of up to one equivalent of $[2\text{Fe-2S}] \text{GRX5}_2$, the fraction of the equivalents of added $[2\text{Fe-2S}] \text{GRX5}_2$ that become apo upon interaction with BOLA1 forms an apo complex with ^{15}N -BOLA3, that is still present in solution at these protein ratios. Also the fraction of uncomplexed ^{15}N -BOLA1, which is also still present at these protein ratios, shows chemical shifts changes in a fast exchange regime on the NMR time scale, indicating the formation of apo BOLA1-GRX5 complex (**Figure S5**). However, upon further additions of $[2\text{Fe-2S}] \text{GRX5}_2$, the formation also of the $[2\text{Fe-2S}] \text{GRX5-BOLA3}$ complex is observed, as demonstrated by the broadening beyond detection of backbone NHs of the Cys binding loop residues, which is determined by paramagnetic effects of $[2\text{Fe-2S}]$ cluster binding. The formation of the $[2\text{Fe-2S}] \text{GRX5-BOLA3}$ complex is complete once a further equivalent of $[2\text{Fe-2S}] \text{GRX5}_2$ was added, i.e. the stoichiometric amount needed to form both BOLAs-GRX5 complexes (**Figure S5**). These data therefore showed that i) the formation of the $[2\text{Fe-2S}] \text{BOLA1-GRX5}$ and $[2\text{Fe-2S}] \text{BOLA3-GRX5}$ complexes is favored with respect to the homodimeric $[2\text{Fe-2S}] \text{GRX5}_2$, and ii) $[2\text{Fe-2S}]$ cluster binding is the driving force that discriminate between the formation of the two heterodimeric complexes, i.e. $[2\text{Fe-2S}] \text{GRX5-BOLA1}$ complex is preferentially formed to the detriment of $[2\text{Fe-2S}] \text{GRX5-BOLA3}$ formation, once there is no enough amount of $[2\text{Fe-2S}] \text{GRX5}_2$ for the formation of both complexes. We can therefore conclude that the $[2\text{Fe-2S}] \text{GRX5-BOLA1}$ complex shows a higher intrinsic stability than the $[2\text{Fe-2S}] \text{GRX5-BOLA3}$ complex.

Our previous work [15] showed that yeast Grx5 is (at least) 4-fold more abundant than BolA1 and BolA3 yeast proteins in yeast mitochondria. Therefore, assuming that similar protein level ratios are also present in human mitochondria (a good approximation given the conservation of the mitochondrial Fe/S machinery throughout all the kingdoms of life) a significant amount of $[2\text{Fe-2S}] \text{GRX5}_2$ is present in the cell, in addition to its smaller fraction

complexed with mitochondrial BOLAs to form the [2Fe-2S] heterodimers. This implies that [2Fe-2S] GRX5₂ is still available at the cellular level to act in cluster transfer to apo proteins, consistent with the proposed Fe/S cluster transfer role of mitochondrial monothiol glutaredoxins [30,46,47]. We cannot, however, exclude that GRX5 versus BOLA1/BOLA3 ratio might be drastically affected in response to different cellular iron concentrations and other cell stress conditions. This is indeed what has been recently found for cytosolic human BOLA2 protein that, in response to increasing iron levels, quantitatively forms a [2Fe-2S] heterocomplex with human GRX3 in human cells, while the cluster-bridged GRX3 homodimers do not accumulate in cultured cells [48].

3.4 Structural models of [2Fe-2S] BOLA1-GRX5 and [2Fe-2S] BOLA3-GRX5

The structural models of the [2Fe-2S] BOLA1-GRX5 and [2Fe-2S] BOLA3-GRX5 complexes were calculated following the standard protocol of HADDOCK 2.1 docking program and using experimental chemical shift mapping data, which provide the identification of the interacting residues in the complex (see section 2.5 for details). HADDOCK calculations were also exploited to discriminate about the most favored tautomeric conformation adopted by the His residues coordinating the cluster (see section 2.5 for details). It appears that N δ 1 of His 67 and N ϵ 2 His 102 in the [2Fe-2S] BOLA1-GRX5 complex and N δ 1 of His 96 in [2Fe-2S] BOLA3-GRX5 complex coordinate iron. The best scoring HADDOCK structural models for each heterocomplex were then refined through AMBER calculations, using, for the cluster moiety and its ligands, force field parameters derived from an oxidized [2Fe-2S]²⁺ cluster for BOLA3-GRX5 complex and from a reduced [2Fe-2S]¹⁺ cluster for BOLA1-GRX5 complex.

From the backbone superimposition of the structures of BOLAs and apo GRX5 with those in the structural models of the [2Fe-2S] BOLAs-GRX5 complexes (**Figure S6**), it results that the major structural rearrangement upon dimer formation and cluster binding involve the

loop region between $\beta 1$ and $\beta 2$ of BOLA3. This is the key region differentiating BolA1-like subfamily from BOLA3-like subfamily at the structural level [15]. Remarkably, this loop of BOLA3, containing the cluster ligand Cys 59, moves closer to the invariant C-terminal His 96 to coordinate the [2Fe-2S] cluster ($S_{\gamma}(\text{Cys59})-\text{N}\delta 1(\text{His96})$ distance changes from 12 Å to 6.5 Å from the free BOLA3 protein to the heterocomplex, **Figure S6**). On the contrary, the regions of the His ligands in BOLA1 do not show large structural rearrangements upon heterocomplex formation and a structural proximity ($\text{N}_{\epsilon 1}(\text{His58})-\text{Fe}(2\text{Fe-2S})$ distance is 4.9 Å) of His 58 to the [2Fe-2S] cluster is observed (**Figure S6**), in agreement with the spectroscopic data that indicate a possible replacement of His 67 by His 58 as cluster ligand, once His 67 was mutated. Comparing the structural model of [2Fe-2S]¹⁺ BOLA1-GRX5 with that of [2Fe-2S]²⁺ BOLA3-GRX5, it results that BOLA1 has a different orientation respect to BOLA3, once the GRX5 structure is superimposed in the two heterocomplexes. This structural difference causes a change in the cluster surface exposure (**Figure 8**). Cluster solvent accessibility increases indeed from 3% to 20% going from the BOLA1 to the BOLA3 heterocomplex. Specifically, in the [2Fe-2S] BOLA1-GRX5 complex, BOLA1 and GRX5 proteins are oriented such that the β -sheet of BOLA1 is at the protein-protein interface embracing both iron atoms of the [2Fe-2S] cluster towards the interior (**Figure 8**). Only through a major structural rearrangement at the protein-protein interface the iron atoms of the cluster might be exposed to the solvent in order to be possibly participate to cluster ligand-exchange reactions with a [2Fe-2S] receiving protein. On the contrary, only the last β -strand of the BOLA3 β -sheet is at the interface with GRX5 in the [2Fe-2S] BOLA3-GRX5 complex, so that the [2Fe-2S] cluster is more accessible on the protein surface (**Figure 8**). The loop containing Cys 69 in BOLA3 can be considered as a gate regulating the [2Fe-2S] cluster access for a [2Fe-2S] receiving protein. Indeed, just a slight movement of this loop (**Figure S6**), possibly determined by the interaction with a [2Fe-2S] receiving protein, can

largely expose one of the iron atoms of the [2Fe-2S] cluster to the solvent, thus easily making it accessible for ligand invasion by the [2Fe-2S] receiving protein. Comparing the two heterodimeric [2Fe-2S] complexes with the homodimeric [2Fe-2S] GRX5₂ complex, it results that the latter shows an elongated shaped structure at variance with the two BOLA3-GRX5 and BOLA1-GRX5 complexes, which are more compact, with BOLA1-GRX5 complex being more compact than BOLA3-GRX5. This determines a higher solvent accessibility of the [2Fe-2S] cluster in the homodimeric GRX5 complex with respect to of both heterocomplexes, in agreement with the general function of GRX5 in transferring [2Fe-2S] clusters to several partners [30,49,50].

4. Conclusions

The different structural and redox properties observed for the two [2Fe-2S] BOLAs-GRX5 complexes as well as their different stability suggest that they have a diverse molecular function. The redox active cluster properties, the high stability and low solvent cluster accessibility found for the [2Fe-2S] BOLA1-GRX5 complex suggests that the latter complex might work in electron transfer reactions. On the contrary, the BOLA3-GRX5 complex, which has a more accessible cluster with no sizable redox properties and with a less stabilized [2Fe-2S] cluster binding (i.e. more prone to be released) can be involved in iron-sulfur cluster transfer processes versus other client proteins along the Fe/S protein assembly pathway. According to its molecular function in [2Fe-2S] cluster transfer processes, the [2Fe-2S] GRX5 and BOLA3 interaction is kinetically labile, especially in the absence of GSH, at variance with what observed for the [2Fe-2S] BOLA1-GRX5 complex [15].

The distinct molecular function that we propose for the two BOLAs complexes is in accordance the functional data reported by Willems et al. 2013 [20]. In this work, it was showed that i) ablation of BOLA1 in cultured human cells increases mitochondrial protein

thiol oxidation and elicits alterations in mitochondrial morphology, ii) BOLA1 overexpression prevents mitochondrial morphology aberrations induced by GSH depletion, iii) the reducing agent DTT, similarly to BOLA1 overexpression, prevents mitochondrial shape changes, while BOLA3 does not result in the same mitochondrial rescue. Specifically, the latter data support that the molecular function of human BOLA1 is different from that of human BOLA3, suggesting that BOLA1 can work as an electron donor, similarly to the DTT reducing agent. The mechanism by which human BOLA1 is specifically regulating mitochondrial thiol redox potential is still unknown. However, since BOLA1 has been shown to interact with GRX5 in mitochondria [20] and yeast BolA1 has been implicated in the late steps of the mitochondrial Fe/S cluster assembly pathway [15,16], we believe that the increased mitochondrial protein thiol oxidation observed upon BOLA1 ablation is an indirect effect of the inability to assemble Fe/S clusters in mitochondria.

In yeast, it has been shown that the cellular function of the two mitochondrial yeast BolAs in the Fe/S cluster assembly pathway is overlapping [15]. However, their function is not entirely identical, as indeed it has been shown that i) small effects occur on lipoic acid synthase and succinate dehydrogenase in *bol3Δ* yeast cells, versus no detectable alterations upon BolA1 deletion; ii) double deletion of BolA3 and Nfu1, encoding another late-acting iron-sulfur cluster assembly factor [16,51], exacerbates the Fe/S protein defects compared to single deletions, while double deletion of BolA1 and Nfu1 behaved similarly to *nfu1Δ* yeast cells [15]. Apparently, even though yeast BolA1 and BolA3 play overlapping roles, their function is not entirely identical. The major evident physiological function, which was observed by double yeast BolA1-BolA3 deletions, is in lipoate synthase maturation and a similar defect is seen in human cells obtained from BOLA3 patients. This phenotype similarity suggests that the yeast mitochondrial BolAs and human BOLA3 are functionally similar, and thus the overlapping function of mitochondrial yeast Bols seems not to be conserved in human BOLA1 and BOLA3, in agreement with the findings of the work by Willems et al. 2013 [20].

In conclusion, our data support a different function of the two human [2Fe-2S] BOLA1-GRX5, [2Fe-2S] BOLA3-GRX5 heterocomplexes in the late steps of mitochondrial Fe/S cluster assembly, i.e. assisting them through different biochemical reaction, i.e. electron transfer vs. cluster transfer, respectively.

Acknowledgments

This work was supported by iNEXT funded by the Horizon 2020 program of the European Commission (contract number 653706), by the COST Action CA15133 “The Biogenesis of Iron-sulfur Proteins: from Cellular Biology to Molecular Aspects (FeSBioNet)”, and by Instruct, part of the European Strategy Forum on Research Infrastructures (ESFRI), and supported by national member subscriptions. We thank the EU ESFRI Instruct Core Centre CERM-Italy.

Supplementary Material

Supplementary Material includes six figures and three tables and can be found online.

References

- [1] E. Herrero and M.A. de la Torre, Monothiol glutaredoxins: a common domain for multiple functions, *Cell Mol. Life Sci.* 64 (2007) pp. 1518-1530.
- [2] H. Li and C.E. Outten, Monothiol CGFS glutaredoxins and BolA-like proteins: [2Fe-2S] binding partners in iron homeostasis, *Biochemistry* 51 (2012) pp. 4377-4389.
- [3] C.C. Philpott, Coming into view: eukaryotic iron chaperones and intracellular iron delivery, *J. Biol. Chem.* 287 (2012) pp. 13518-13523.
- [4] M.A. Huynen, C.A. Spronk, T. Gabaldon, B. Snel, Combining data from genomes, Y2H and 3D structure indicates that BolA is a reductase interacting with a glutaredoxin, *FEBS Lett.* 579 (2005) pp. 591-596.
- [5] J. Couturier, J. Przybyla-Toscano, T. Roret, C. Didierjean, N. Rouhier, The roles of glutaredoxins ligating Fe-S clusters: Sensing, transfer or repair functions?, *Biochim. Biophys. Acta* 1853 (2015) pp. 1513-1527.
- [6] T.A. Rouault, Mammalian iron-sulphur proteins: novel insights into biogenesis and function, *Nat. Rev. Mol. Cell Biol* 16 (2015) pp. 45-55.
- [7] X. Nuttle, G. Giannuzzi, M.H. Duyzend, J.G. Schraiber, I. Narvaiza, F. Camponeschi, S. Ciofi-Baffoni, P.H. Sudmant, O. Penn, G. Chiatante, M. Malig, J. Huddleston, C. Benner, H.A.F. Stessman, M.C.N. Marchetto, L. Denman, L. Harshman, C. Baker, A. Raja, K. Penewit, W.J. Tang, M. Ventura, F. Antonacci, J.M. Akey, C.T. Amemiya, L. Banci, F.H. Gage, A. Reymond, E.E. Eichler, Emergence of a *Homo sapiens*-specific gene family and the evolution of autism risk at chromosome 16p11.2, *Nature* 536 (2016) pp. 205-209.

- [8] C. Andreini, L. Banci, A. Rosato, Exploiting bacterial operons to illuminate human iron-sulfur proteins, *J. Proteome Res.* 15 (2016) pp. 1308-1322.
- [9] J. Couturier, J.P. Jacquot, N. Rouhier, Evolution and diversity of glutaredoxins in photosynthetic organisms, *Cell Mol. Life Sci.* 66 (2009) pp. 2539-2557.
- [10] A. Kumanovics, O.S. Chen, L. Li, D. Bagley, E.M. Adkins, H. Lin, N.N. Dingra, C.E. Outten, G. Keller, D. Winge, D.M. Ward, J. Kaplan, Identification of FRA1 and FRA2 as genes involved in regulating the yeast iron regulon in response to decreased mitochondrial iron-sulfur cluster synthesis, *J. Biol Chem* 283 (2008) pp. 10276-10286.
- [11] C.B. Poor, S.V. Wegner, H. Li, A.C. Dlouhy, J.P. Schuermann, R. Sanishvili, J.R. Hinshaw, P.J. Riggs-Gelasco, C.E. Outten, C. He, Molecular mechanism and structure of the *Saccharomyces cerevisiae* iron regulator Aft2, *Proc. Natl. Acad. Sci. USA* 111 (2014) pp. 4043-4048.
- [12] L. Banci, F. Camponeschi, S. Ciofi-Baffoni, R. Muzzioli, Elucidating the molecular function of human BOLA2 in GRX3-Dependent anamorsin maturation pathway, *J. Am. Chem. Soc.* 137 (2015) pp. 16133-16134.
- [13] L. Banci, S. Ciofi-Baffoni, K. Gajda, R. Muzzioli, R. Peruzzini, J. Winkelmann, N-terminal domains mediate [2Fe-2S] cluster transfer from glutaredoxin-3 to anamorsin, *Nat. Chem Biol* 11 (2015) pp. 772-778.
- [14] A.G. Frey, D.J. Palenchar, J.D. Wildemann, C.C. Philpott, A Glutaredoxin-BolA Complex Serves as an Iron-Sulfur Cluster Chaperone for the Cytosolic Cluster Assembly Machinery, *J. Biol Chem* (2016).

- [15] M.A. Uzarska, V. Nasta, B.D. Weiler, F. Spantgar, S. Ciofi-Baffoni, M. Saviello, L. Gonnelli, U. Muhlenhoff, L. Banci, R. Lill, Mitochondrial Bol1 and Bol3 function as assembly factors for specific iron-sulfur proteins, *Elife* 5 (2016) p.e16673.
- [16] A. Melber, U. Na, A. Vashisht, B.D. Weiler, R. Lill, J.A. Wohlschlegel, D.R. Winge, Role of Nfu1 and Bol3 in iron-sulfur cluster transfer to mitochondrial clients, *Elife* 5 (2016) p.e15991.
- [17] P.R. Baker, M.W. Friederich, M.A. Swanson, T. Shaikh, K. Bhattacharya, G.H. Scharer, J. Aicher, G. Creadon-Swindell, E. Geiger, K.N. MacLean, W.T. Lee, C. Deshpande, M.L. Freckmann, L.Y. Shih, M. Wasserstein, M.B. Rasmussen, A.M. Lund, P. Procopis, J.M. Cameron, B.H. Robinson, G.K. Brown, R.M. Brown, A.G. Compton, C.L. Dieckmann, R. Collard, C.R. Coughlin, E. Spector, M.F. Wempe, J.L. Van Hove, Variant non ketotic hyperglycinemia is caused by mutations in LIAS, BOLA3 and the novel gene GLRX5, *Brain* 137 (2014) pp. 366-379.
- [18] J.M. Cameron, A. Janer, V. Levandovskiy, N. MacKay, T.A. Rouault, W.H. Tong, I. Ogilvie, E.A. Shoubridge, B.H. Robinson, Mutations in iron-sulfur cluster scaffold genes NFU1 and BOLA3 cause a fatal deficiency of multiple respiratory chain and 2-oxoacid dehydrogenase enzymes, *Am. J. Hum. Genet.* 89 (2011) pp. 486-495.
- [19] T.B. Haack, B. Rolinski, B. Haberberger, F. Zimmermann, J. Schum, V. Strecker, E. Graf, U. Athing, T. Hoppen, I. Wittig, W. Sperl, P. Freisinger, J.A. Mayr, T.M. Strom, T. Meitinger, H. Prokisch, Homozygous missense mutation in BOLA3 causes multiple mitochondrial dysfunctions syndrome in two siblings, *J. Inherit. Metab Dis.* 36 (2013) pp. 55-62.

- [20] P. Willems, B.F. Wanschers, J. Esseling, R. Szklarczyk, U. Kudla, I. Duarte, M. Forkink, M. Nooteboom, H. Swarts, J. Gloerich, L. Nijtmans, W. Koopman, M.A. Huynen, BOLA1 is an aerobic protein that prevents mitochondrial morphology changes induced by glutathione depletion, *Antioxid. Redox. Signal.* 18 (2013) pp. 129-138.
- [21] N. Yeung, B. Gold, N.L. Liu, R. Prathapam, H.J. Sterling, E.R. Willams, G. Butland, The E. coli monothiol glutaredoxin GrxD forms homodimeric and heterodimeric FeS cluster containing complexes, *Biochemistry* 50 (2011) pp. 8957-8969.
- [22] A.C. Dlouhy, H. Li, A.N. Albetel, B. Zhang, D.T. Mapolelo, S. Randeniya, A.A. Holland, M.K. Johnson, C.E. Outten, The Escherichia coli BolA Protein IbaG Forms a Histidine-Ligated [2Fe-2S]-Bridged Complex with Grx4, *Biochemistry* 55 (2016) pp. 6869-6879.
- [23] T. Roret, P. Tsan, J. Couturier, B. Zhang, M.K. Johnson, N. Rouhier, C. Didierjean, Structural and spectroscopic insights into BolA-glutaredoxin complexes, *J. Biol. Chem.* 289 (2014) pp. 24588-24598.
- [24] T. Dhalleine, N. Rouhier, J. Couturier, Putative roles of glutaredoxin-BolA heterodimers in plants, *Plant Signal. Behav.* 9 (2014) p.e28564.
- [25] J. Couturier, H.C. Wu, T. Dhalleine, H. Pegeot, D. Sudre, J.M. Gualberto, J.P. Jacquot, F. Gaymard, F. Vignols, N. Rouhier, Monothiol glutaredoxin-BolA interactions: redox control of Arabidopsis thaliana BolA2 and SufE1, *Mol. Plant* 7 (2014) pp. 187-205.
- [26] H. Li, D.T. Mapolelo, N.N. Dingra, S.G. Naik, N.S. Lees, B.M. Hoffman, P.J. Riggs-Gelasco, B.H. Huynh, M.K. Johnson, C.E. Outten, The yeast iron regulatory

proteins Grx3/4 and Fra2 form heterodimeric complexes containing a [2Fe-2S] cluster with cysteinyl and histidyl ligation, *Biochemistry* 48 (2009) pp. 9569-9581.

[27] H. Li, D.T. Mapolelo, N.N. Dingra, G. Keller, P.J. Riggs-Gelasco, D.R. Winge, M.K. Johnson, C.E. Outten, Histidine 103 in Fra2 is an iron-sulfur cluster ligand in the [2Fe-2S] Fra2-Grx3 complex and is required for in vivo iron signaling in yeast, *J. Biol Chem* 286 (2011) pp. 867-876.

[28] H. Li, D.T. Mapolelo, S. Randeniya, M.K. Johnson, C.E. Outten, Human glutaredoxin 3 forms [2Fe-2S]-bridged complexes with human BolA2, *Biochemistry* 51 (2012) pp. 1687-1696.

[29] Y.B. Zhou, J.B. Cao, B.B. Wan, X.R. Wang, G.H. Ding, H. Zhu, H.M. Yang, K.S. Wang, X. Zhang, Z.G. Han, hBolA, novel non-classical secreted proteins, belonging to different BolA family with functional divergence, *Mol. Cell Biochem.* 317 (2008) pp. 61-68.

[30] L. Banci, D. Brancaccio, S. Ciofi-Baffoni, R. Del Conte, R. Gadepalli, M. Mikolajczyk, S. Neri, M. Piccioli, J. Winkelmann, [2Fe-2S] cluster transfer in iron-sulfur protein biogenesis, *Proc. Natl. Acad. Sci. USA* 111 (2014) pp. 6203-6208.

[31] C. Johansson, A.K. Roos, S.J. Montano, R. Sengupta, P. Filippakopoulos, K. Guo, F. von Delft, A. Holmgren, U. Oppermann, K.L. Kavanagh, The crystal structure of human GLRX5: iron-sulfur cluster co-ordination, tetrameric assembly and monomer activity, *Biochem. J.* 433 (2011) pp. 303-311.

[32] J. Abendroth, A.S. Gardberg, J.I. Robinson, J.S. Christensen, B.L. Staker, P.J. Myler, L.J. Stewart, T.E. Edwards, SAD phasing using iodide ions in a high-

throughput structural genomics environment, *J. Struct. Funct. Genomics* 12 (2011) pp. 83-95.

- [33] T. Kasai, M. Inoue, S. Koshiba, T. Yabuki, M. Aoki, E. Nunokawa, E. Seki, T. Matsuda, N. Matsuda, Y. Tomo, M. Shirouzu, T. Terada, N. Obayashi, H. Hamana, N. Shinya, A. Tatsuguchi, S. Yasuda, M. Yoshida, H. Hirota, Y. Matsuo, K. Tani, H. Suzuki, T. Arakawa, P. Carninci, J. Kawai, Y. Hayashizaki, T. Kigawa, S. Yokoyama, Solution structure of a BolA-like protein from *Mus musculus*, *Protein Sci.* 13 (2004) pp. 545-548.
- [34] K.H. Chin, F.Y. Lin, Y.C. Hu, K.H. Sze, P.C. Lyu, S.H. Chou, NMR structure note-- solution structure of a bacterial BolA-like protein XC975 from a plant pathogen *Xanthomonas campestris* pv. *campestris*, *J. Biomol. NMR* 31 (2005) pp. 167-172.
- [35] G.W. Buchko, A. Yee, A. Semesi, P.J. Myler, C.H. Arrowsmith, R. Hui, Solution-state NMR structure of the putative morphogene protein BolA (PFE0790c) from *Plasmodium falciparum*, *Acta Crystallogr. F. Struct. Biol Commun.* 71 (2015) pp. 514-521.
- [36] C. Dominguez, R. Boelens, A.M. Bonvin, HADDOCK: a protein-protein docking approach based on biochemical or biophysical information, *J. Am. Chem. Soc.* 125 (2003) pp. 1731-1737.
- [37] D.A. Case, T.A. Darden, T.E. Cheatham, III, C.L. Simmerling, J. Wang, R.E. Duke, R. Luo, R.C. Walker, W. Zhang, K.M. Merz, B. Roberts, S. Hayik, A. Roitberg, G. Seabra, J. Swails, A.W. Goetz, I. Kilossvary, K.F. Wong, F. Paesani, J. Vanicek, R.M. Wolf, J. Liu, X. Wu, S.R. Brozell, T. Steinbrecher, H. Gohlke, Q. Cai, X. Ye, M.-J. Hsieh, G. Cui, D.R. Roe, D.H. Mathews, M.G. Seetin, R.

Salomon-Ferrer, C. Sagui, V. Babin, T. Luchko, S. Gusarov, A. Kovalenko, P.A. Kollman, AMBER 12, University of California, San Francisco, CA, 2012.

- [38] P. Li and K.M. Merz, Jr., MCPB.py: A Python Based Metal Center Parameter Builder, *J. Chem. Inf. Model.* 56 (2016) pp. 599-604.
- [39] B. Xia, D. Jenk, D.M. LeMaster, W.M. Westler, J.L. Markley, Electron-nuclear interactions in two prototypical [2Fe-2S] proteins: selective (chiral) deuteration and analysis of (1)H and (2)H NMR signals from the alpha and beta hydrogens of cysteinyl residues that ligate the iron in the active sites of human ferredoxin and Anabaena 7120 vegetative ferredoxin, *Arch Biochem Biophys* 373 (2000) pp. 328-334.
- [40] L. Banci, I. Bertini, C. Luchinat, The ¹H NMR parameters of magnetically coupled dimers - The Fe₂S₂ proteins as an example, *Struct. Bonding* 72 (1990) pp. 113-135.
- [41] N. Rouhier, J. Couturier, M.K. Johnson, J.P. Jacquot, Glutaredoxins: roles in iron homeostasis, *Trends Biochem. Sci.* 35 (2010) pp. 43-52.
- [42] D.W. Bak and S.J. Elliott, Alternative FeS cluster ligands: tuning redox potentials and chemistry, *Curr. Opin. Chem Biol* 19 (2014) pp. 50-58.
- [43] M.E. Anderson, Determination of glutathione and glutathione disulfide in biological samples, *Methods Enzymol.* 113 (1985) pp. 548-555.
- [44] L. Banci, S. Ciofi-Baffoni, M. Mikolajczyk, J. Winkelmann, E. Bill, M.E. Pandelia, Human anamorsin binds [2Fe-2S] clusters with unique electronic properties, *J. Biol. Inorg. Chem.* 18 (2013) pp. 883-893.

- [45] M. Orio and J.M. Mouesca, Variation of average g values and effective exchange coupling constants among [2Fe-2S] clusters: a density functional theory study of the impact of localization (trapping forces) versus delocalization (double-exchange) as competing factors, *Inorg. Chem* 47 (2008) pp. 5394-5416.
- [46] M.A. Uzarska, R. Dutkiewicz, S.A. Freibert, R. Lill, U. Muhlenhoff, The mitochondrial Hsp70 chaperone Ssq1 facilitates Fe/S cluster transfer from Isu1 to Grx5 by complex formation, *Mol. Biol. Cell* 24 (2013) pp. 1830-1841.
- [47] O. Stehling, C. Wilbrecht, R. Lill, Mitochondrial iron-sulfur protein biogenesis and human disease, *Biochimie* 100 (2014) pp. 61-77.
- [48] A.G. Frey, D.J. Palenchar, J.D. Wildemann, C.C. Philpott, A Glutaredoxin-BolA Complex Serves as an Iron-Sulfur Cluster Chaperone for the Cytosolic Cluster Assembly Machinery, *J. Biol Chem* (2016).
- [49] D. Brancaccio, A. Gallo, M. Mikolajczyk, K. Zovo, P. Palumaa, E. Novellino, M. Piccioli, S. Ciofi-Baffoni, L. Banci, Formation of [4Fe-4S] clusters in the mitochondrial iron-sulfur cluster assembly machinery, *J. Am. Chem Soc.* 136 (2014) pp. 16240-16250.
- [50] B. Zhang, S. Bandyopadhyay, P. Shakamuri, S.G. Naik, B.H. Huynh, J. Couturier, N. Rouhier, M.K. Johnson, Monothiol glutaredoxins can bind linear [Fe₃S₄]⁺ and [Fe₄S₄]²⁺ clusters in addition to [Fe₂S₂]²⁺ clusters: spectroscopic characterization and functional implications, *J. Am. Chem Soc.* 135 (2013) pp. 15153-15164.
- [51] A. Navarro-Sastre, F. Tort, O. Stehling, M.A. Uzarska, J.A. Arranz, T.M. Del, M.T. Labayru, J. Landa, A. Font, J. Garcia-Villoria, B. Merinero, M. Ugarte, L.G.

Gutierrez-Solana, J. Campistol, A. Garcia-Cazorla, J. Vaquerizo, E. Riudor, P. Briones, O. Elpeleg, A. Ribes, R. Lill, A fatal mitochondrial disease is associated with defective NFU1 function in the maturation of a subset of mitochondrial Fe-S proteins, *Am. J. Hum. Genet.* 89 (2011) pp. 656-667.

Figure Legends

Figure 1. EPR and paramagnetic ^1H NMR spectra of [2Fe-2S] GRX5-BOLA3 and [2Fe-2S] GRX5-BOLA1 complexes. EPR spectra at 45 K recorded on chemically reconstituted [2Fe-2S] GRX5-BOLA3 (**A**) and [2Fe-2S] GRX5-BOLA1 (**B**) complexes, before (black line) and after (red line) anaerobic reduction with stoichiometric amounts of sodium dithionite and rapid freezing. The g-values were calculated using microwave frequencies 9.401 and 9.422 MHz, respectively. Paramagnetic ^1H NMR spectra of chemically reconstituted [2Fe-2S] GRX5-BOLA3 (**C**) and [2Fe-2S] GRX5-BOLA1 (**D**) complexes recorded at 283 K and 600 MHz. Recycle times are 93 ms and 285 ms, respectively. In the inset, the low-field region of the paramagnetic ^1H NMR spectrum of the chemically reconstituted [2Fe-2S] GRX5-BOLA1, obtained with a faster recycle time of 33 ms, is shown. The signals of a small fraction of oxidized cluster $[\text{2Fe-2S}]^{2+}$ is indicated as Ox in the spectrum.

Figure 2. Monitoring cluster binding by UV/vis spectroscopy. (**A**) UV/vis absorption spectra of [2Fe-2S] BOLA3-GRX5 (red line) and [2Fe-2S] C59A BOLA3-GRX5 (black line); (**B**) and of [2Fe-2S] BOLA1-GRX5 (red line), [2Fe-2S] H58A BOLA1-GRX5 (black line), [2Fe-2S] H67A BOLA1-GRX5 (green line). ϵ values are based on the [2Fe-2S] cluster concentration.

Figure 3. Monitoring cluster binding by CD spectroscopy. CD spectra of (**A**) [2Fe-2S] BOLA1-GRX5, [2Fe-2S] H58A BOLA1-GRX5, [2Fe-2S] H67A BOLA1-GRX5, and of (**B**) [2Fe-2S] BOLA1-GRX5, [2Fe-2S] C59A BOLA1-GRX5 in 50 mM phosphate buffer in the presence or not of 5 mM DTT and 5 mM GSH are shown. $\Delta\epsilon$ values are based on the [2Fe-2S] concentration.

Figure 4. C59A BOLA3, H58A or H67A BOLA1 mutation effects on BOLAs structures. On the left panels, backbone weighted average chemical shift differences $\Delta_{\text{avg}}(\text{HN})$ (i.e.

$\left(\frac{((\Delta H)^2 + (\Delta N/5)^2)/2}{2}\right)^{1/2}$, between wt BOLA3 and C59A BOLA3 mutant (**A**), and between wt BOLA1 and H58A (**B**) or H67A (**C**) BOLA1 mutants are shown. The indicated threshold values (obtained by averaging $\Delta_{\text{avg}}(\text{HN})$ values plus 1σ) were used to define meaningful chemical shift differences. On the right panels, the residues experiencing meaningful chemical shift differences were mapped in red on the solution structures of wt BOLAs. Conserved His and Cys residues potentially involved in cluster binding are indicated.

Figure 5. Mapping BOLA3 interacting interface in BOLA3-GRX5 and C59A BOLA3-GRX5 complexes by NMR. Residues experiencing meaningful chemical shift $\Delta_{\text{avg}}(\text{HN})$ differences were obtained comparing i) the ^1H - ^{15}N HSQC spectrum of BOLA3 or C59A BOLA3 with that of apo BOLA3-GRX5 or apo C59A BOLA3-GRX5 complex, respectively; ii) the ^1H - ^{15}N HSQC spectrum of apo BOLA3-GRX5 or apo C59A BOLA3-GRX5 complex before and after the addition of 5 mM GSH; iii) the ^1H - ^{15}N HSQC spectrum of apo BOLA3-GRX5 or apo C59A BOLA3-GRX5 complex before and after [2Fe-2S] cluster binding. The identified residues are mapped on the solution structure of BOLA3 in (**A**), (**B**), and (**C**), respectively. Color codes: in green, residues showing meaningful chemical shift changes; in red, residues broaden beyond detection; residues in green or in red in the **A** or **B** panels are in blue in the **B** or **C** panels, respectively. Cys 59 and His 96 residues are indicated as yellow and blue sticks, respectively.

Figure 6. Mapping BOLA1 interacting interface in BOLA1-GRX5, H58A BOLA1-GRX5 and H67A BOLA1-GRX5 complexes by NMR. (**A**) Residues experiencing meaningful chemical shift $\Delta_{\text{avg}}(\text{HN})$ differences were obtained comparing i) the ^1H - ^{15}N HSQC spectrum of BOLA1 or H58A BOLA1 or H67A BOLA1 with that of apo BOLA1-GRX5 or apo H58A BOLA1-GRX5 or H67A BOLA1-GRX5 complex, respectively; (**B**) the ^1H - ^{15}N HSQC spectrum of apo BOLA1-GRX5 or apo H58A BOLA1-GRX5 or H67A BOLA1-GRX5 complex before and after the addition of 5 mM GSH; (**C**) the ^1H - ^{15}N HSQC spectrum of apo BOLA1-

GRX5 or apo H58A BOLA1-GRX5 or H67A BOLA1-GRX5 complex before and after [2Fe-2S] cluster binding. The identified residues are mapped on the solution structure of BOLA1 in (A), (B), and (C), respectively. Color codes: in green, residues showing meaningful chemical shift changes; in red, residues broadened beyond detection; the residues in green or in red in A or B panel are in blue in the B or C panel, respectively, with the exception of those residues which from chemical shift fast exchange show broaden beyond detection effects upon GSH addition or [2Fe-2S] binding; the latter residues are in red. His 58, His 67 and His 102 residues are indicated as blue sticks.

Figure 7. EPR spectra of mutant BOLA1-GRX5 and BOLA3-GRX5 heterocomplexes.

EPR spectra at 45 K of chemically reconstituted (A) [2Fe-2S] C59A BOLA3-GRX5, (B) [2Fe-2S] H67A BOLA1-GRX5, and (C) [2Fe-2S] H58A BOLA1-GRX5 before (black line) and after (red line) anaerobic reduction with stoichiometric sodium dithionite and rapid freezing. The g-values were calculated using microwave frequencies 9.380, 9.422, and 9.419 MHz, respectively.

Figure 8. Structural models of [2Fe-2S]²⁺ BOLA3-GRX5 and [2Fe-2S]¹⁺ BOLA1-GRX5 complexes.

The structural models of the [2Fe-2S]²⁺ BOLA3-GRX5 and [2Fe-2S]¹⁺ BOLA1-GRX5 complexes are shown in two different orientations. GRX5, BOLA3 and BOLA1 structures are in red, cyano and green, respectively. The invariant C-terminal His (His 96 in BOLA3 and His 102 in BOLA1), His 67 in BOLA1, Cys 59 in BOLA3, Cys 67 in GRX5 residues and GSH involved in cluster binding are shown.

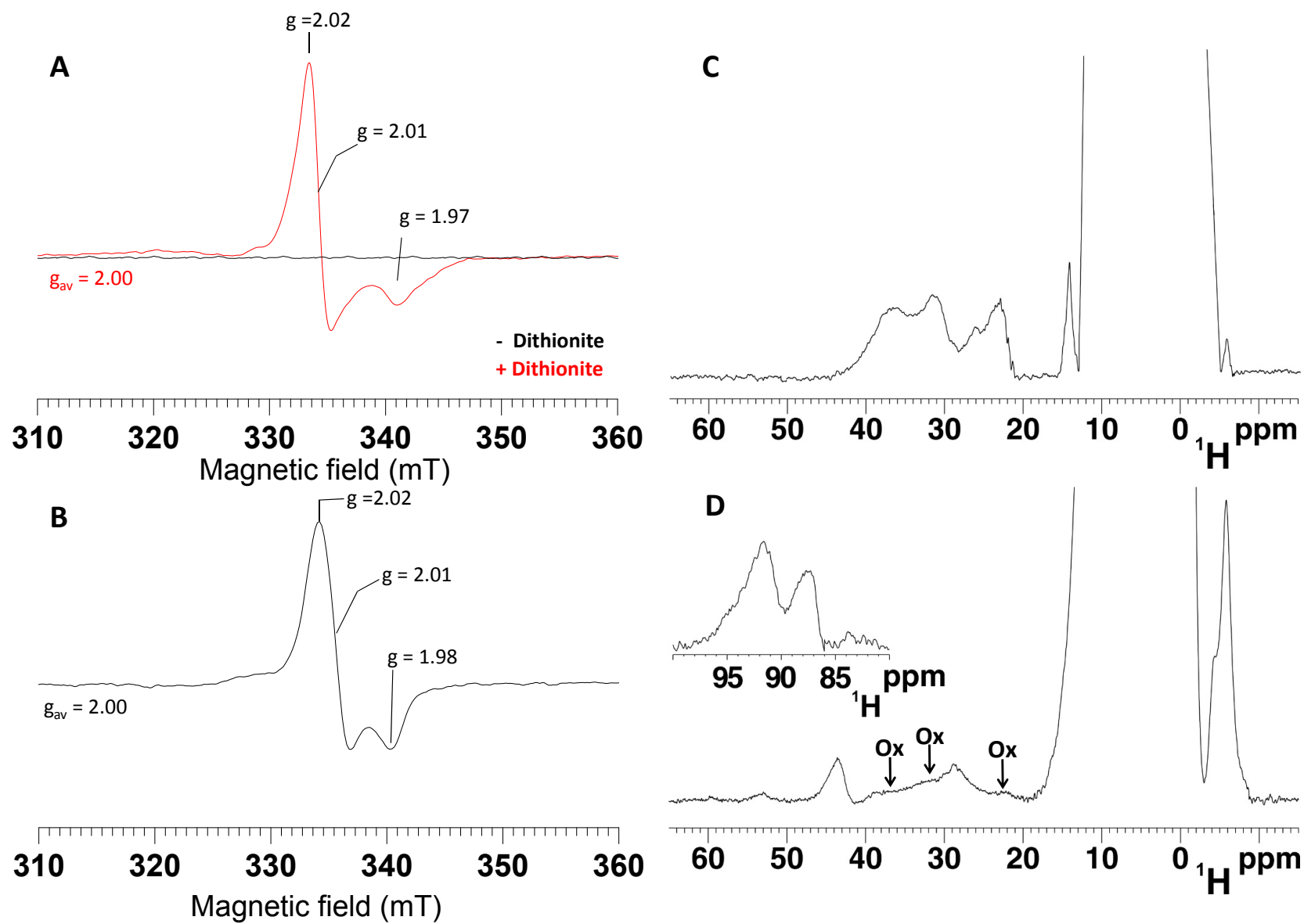


Figure 1

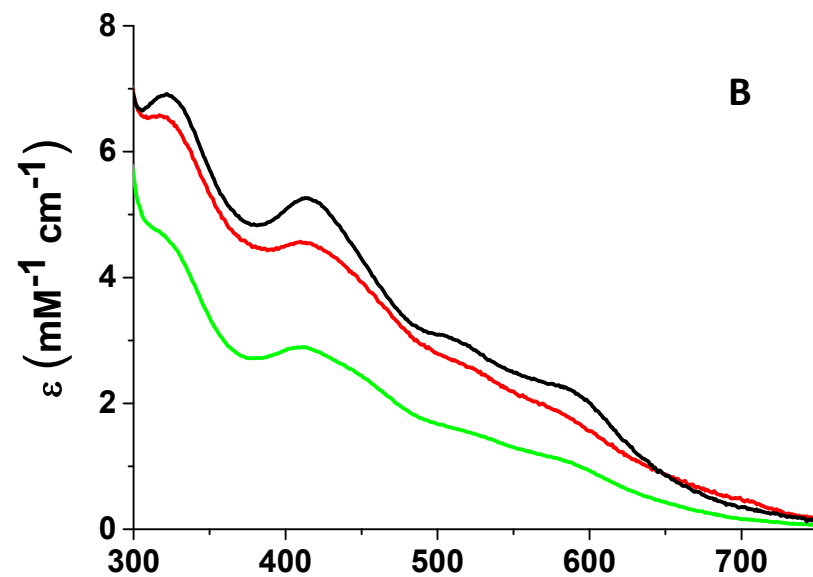
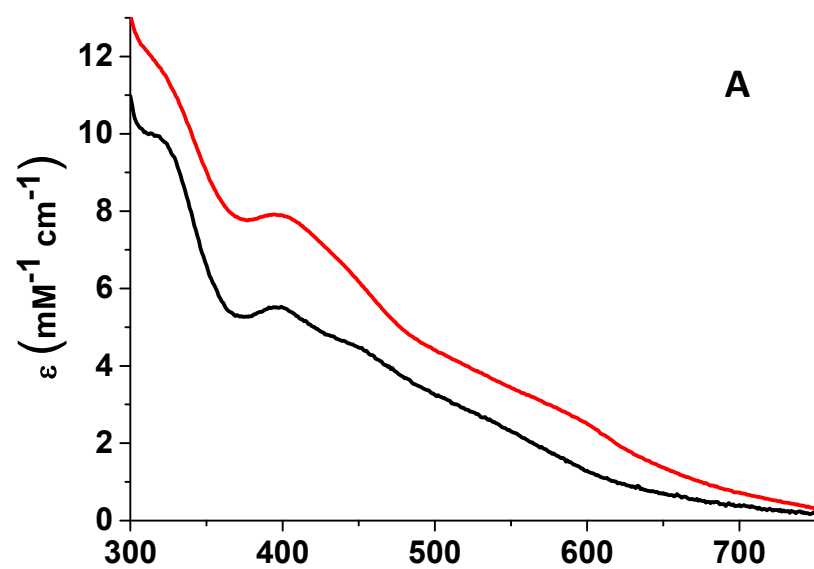


Figure 2

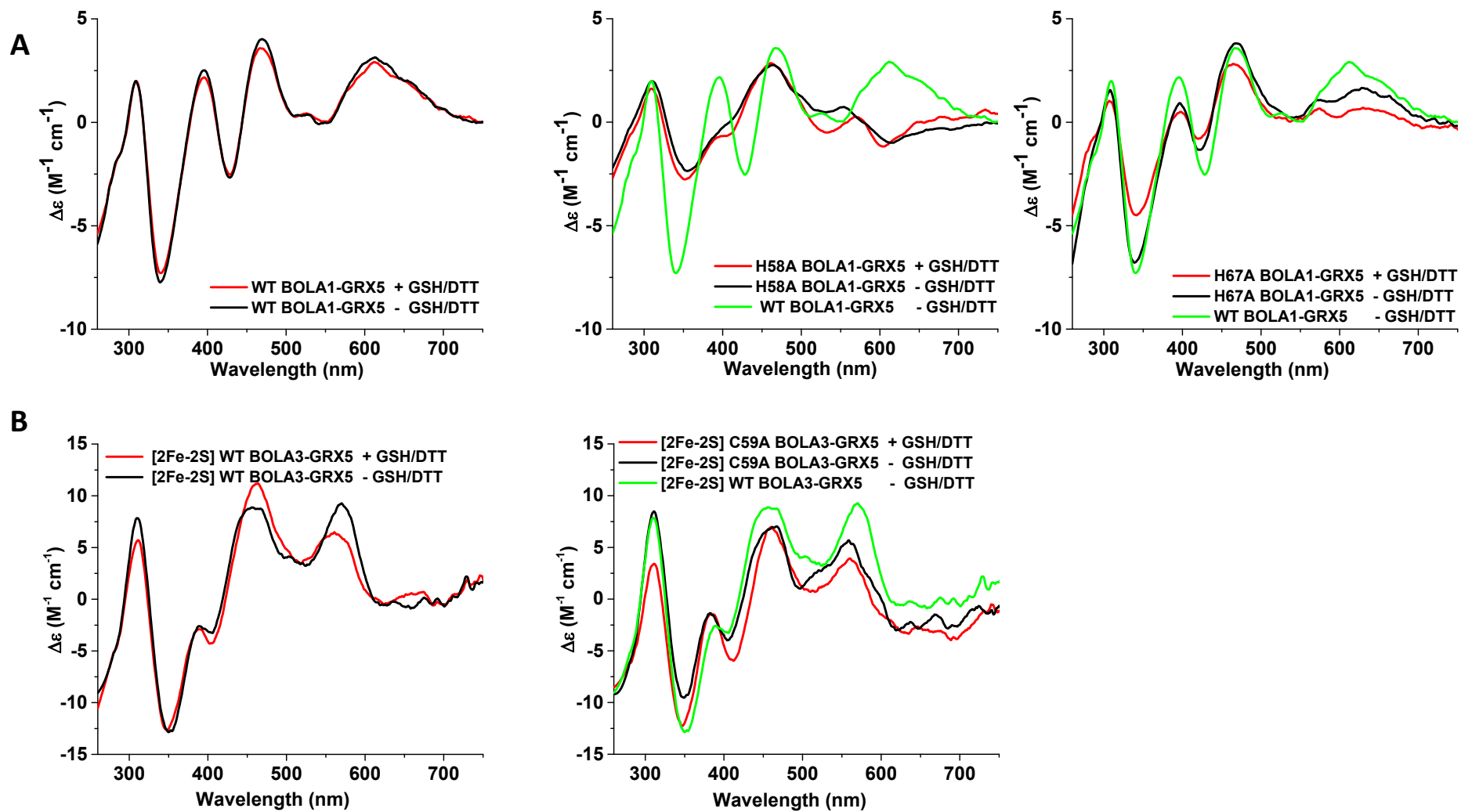


Figure 3

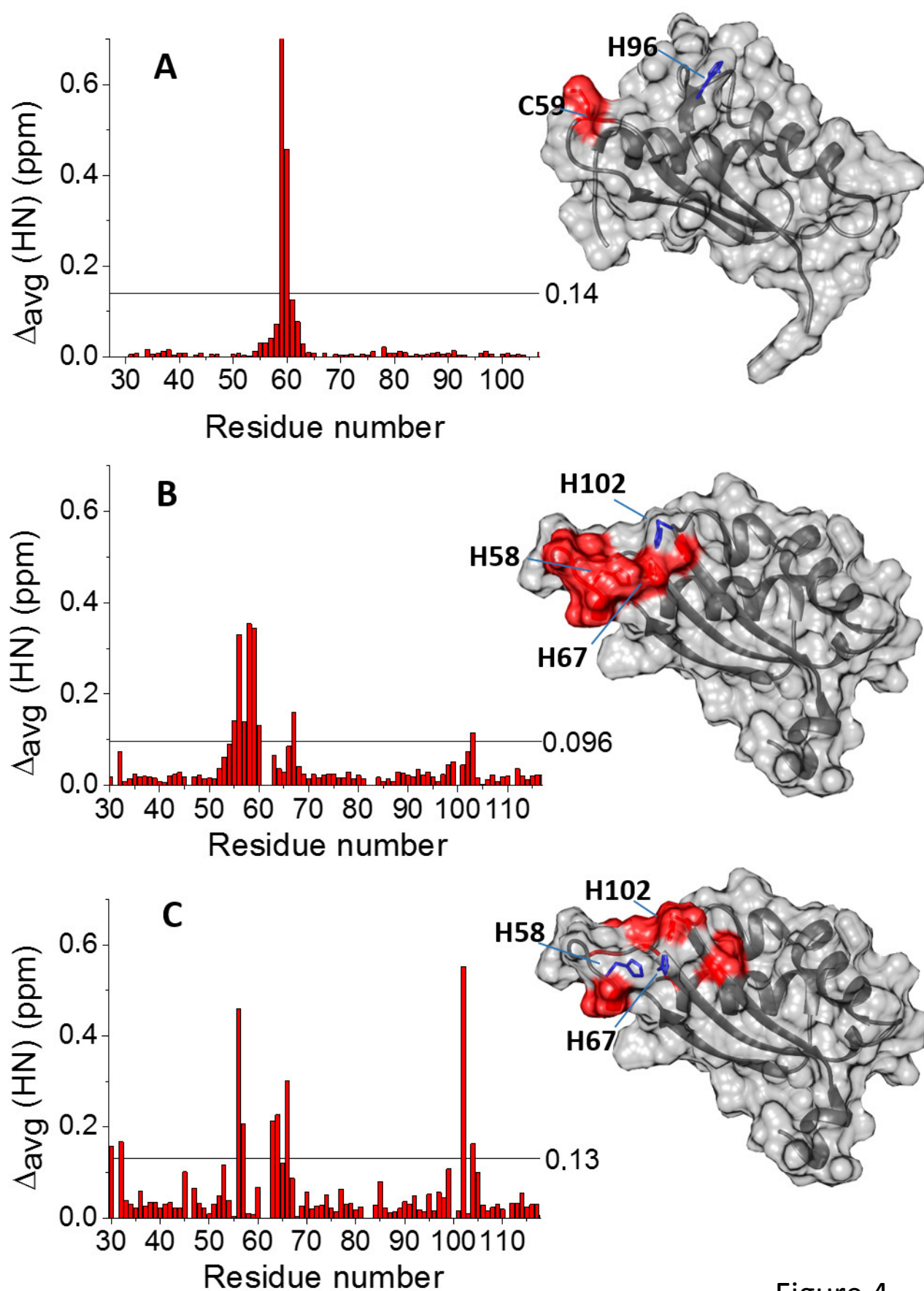


Figure 4

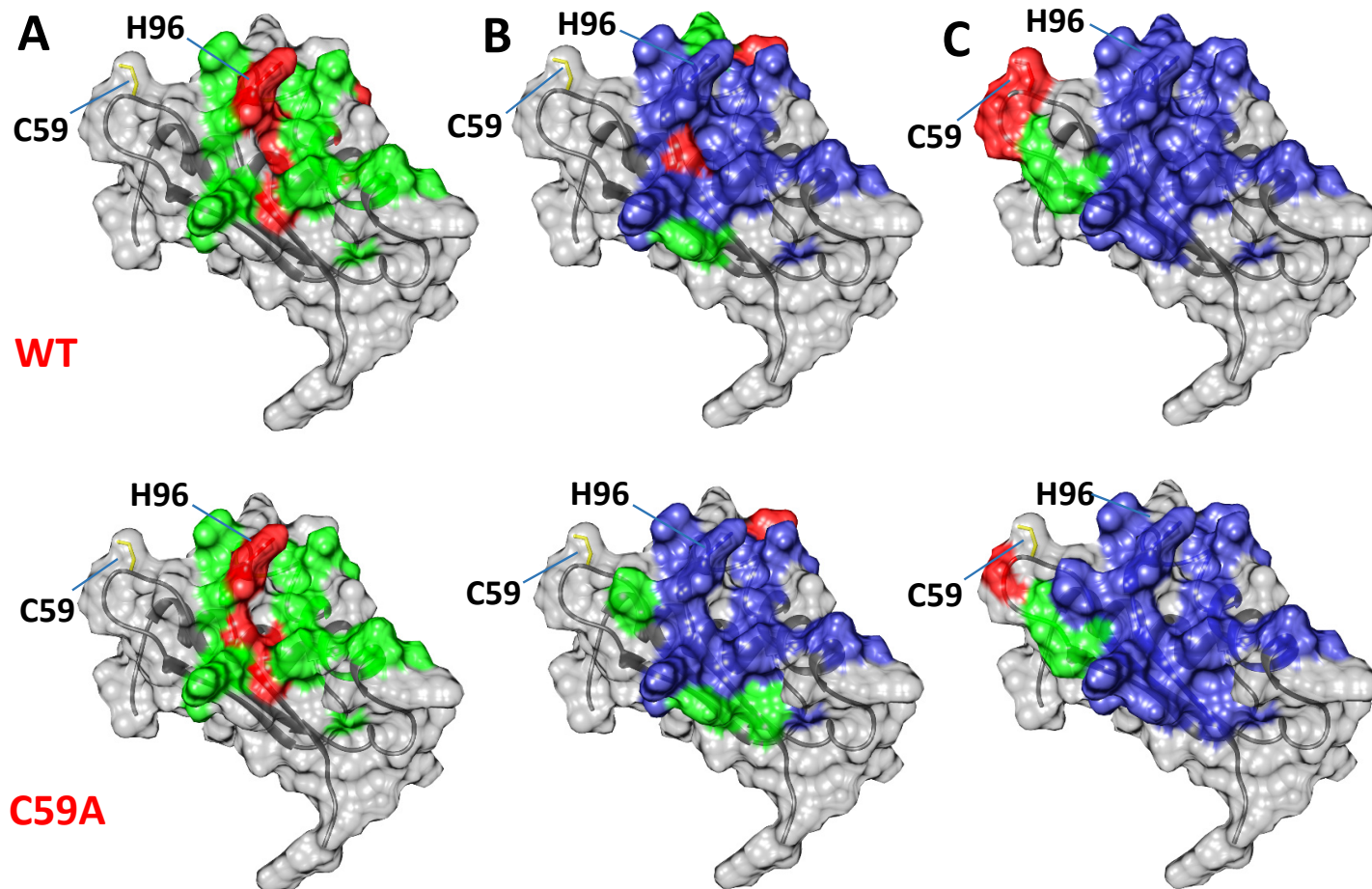


Figure 5

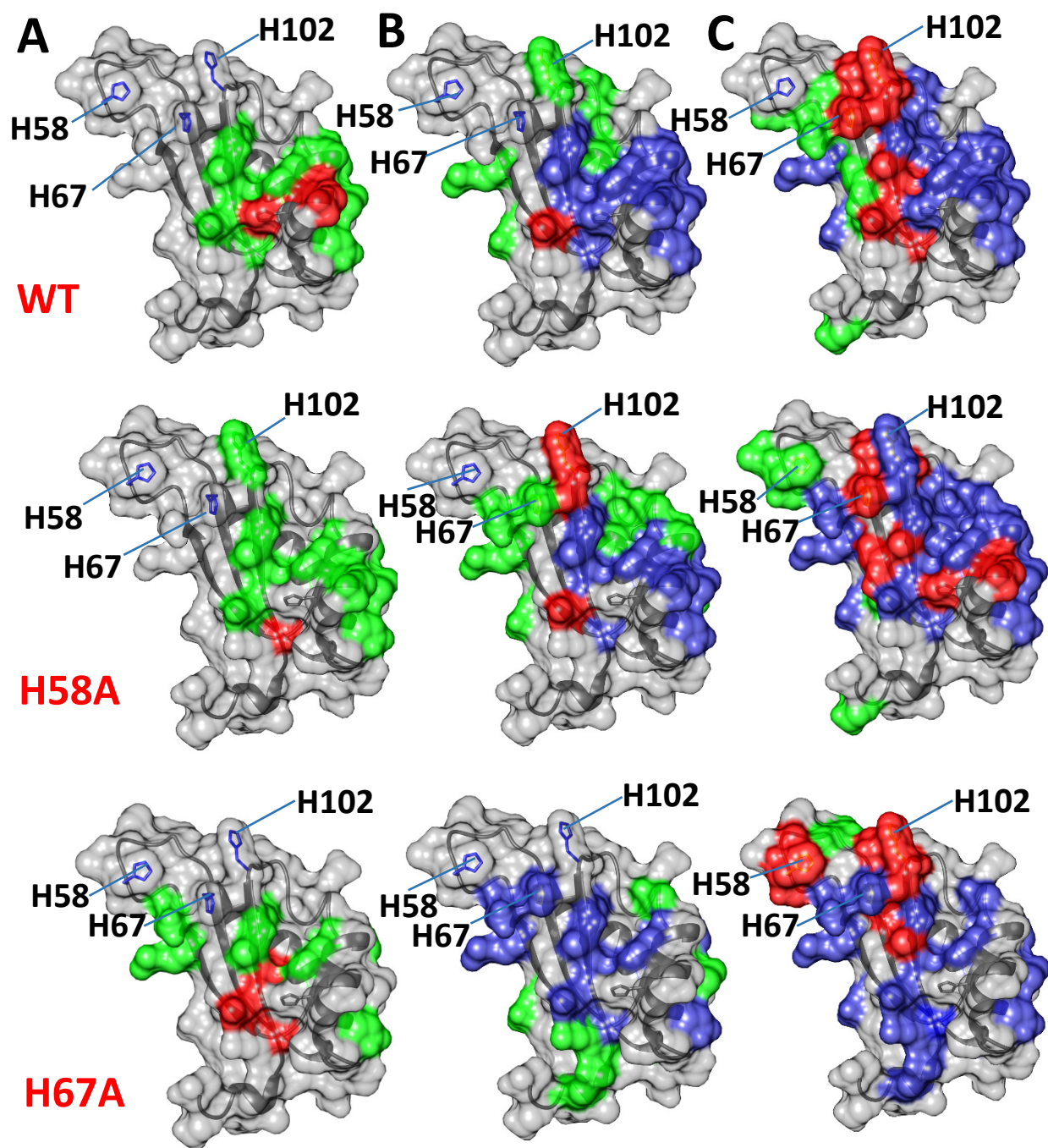


Figure 6

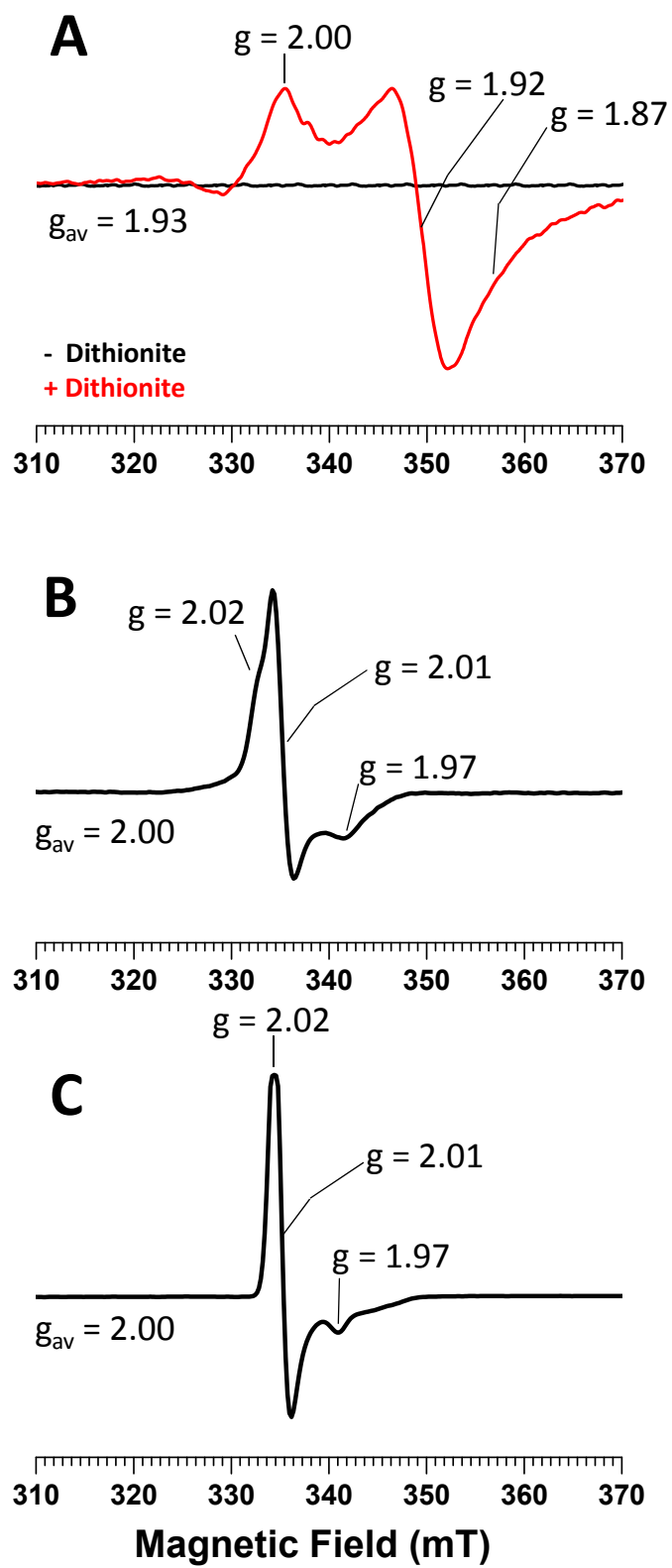


Figure 7

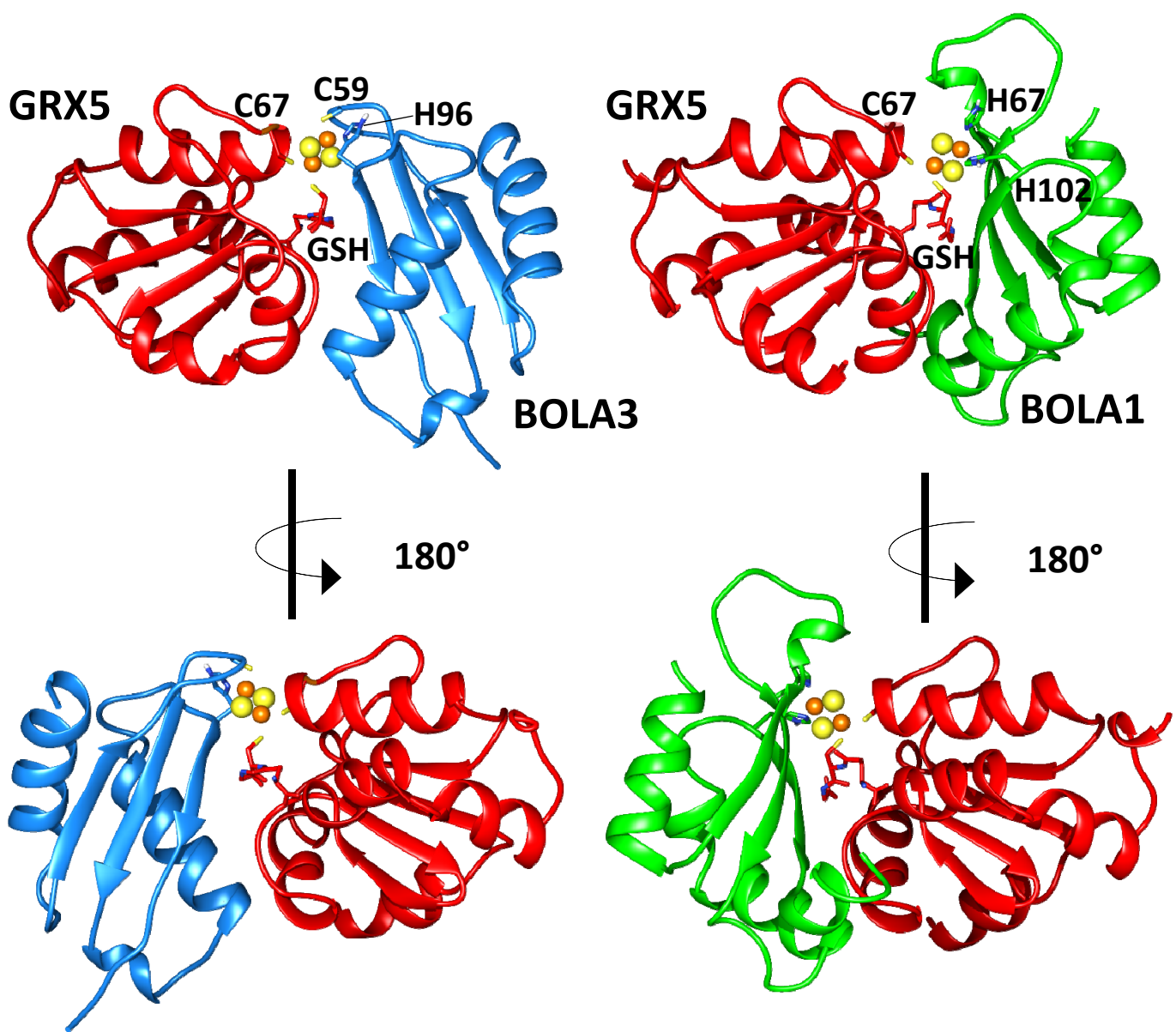


Figure 8